1

New Directions in the Dynamic Assessment of Brain Blood Flow Regulation

Christopher K. Willie, Lindsay K. Eller and Philip N. Ainslie
School of Health and Exercise Sciences, Faculty of Health and Social Development, University of British Columbia Okanagan, Canada

1. Introduction

The principal aim of this book chapter is to provide an overview of the utilities of transcranial Doppler ultrasound (TCD), and high resolution vascular ultrasound for the assessment of human cerebrovascular function with respect to other common measurement tools. Specifically, we aim to: (1) examine the advantages and disadvantages of TCD in the context of other imaging metrics; (2) highlight the optimum approaches for insonation of the basal intra-cerebral arteries; (3) provide a detailed summary of the utility of TCD for assessing cerebrovascular reactivity, autoregulation and neurovascular coupling and the clinical application of these measures; (4) give detailed guidelines for the appropriate use and caveats of neck artery flow measures for the assessment of regional cerebral blood flow distribution; and (5) provide recommendations on the integrative assessment of cerebrovascular function. Finally, we provide an overview of new directions for the optimization of TCD and vascular ultrasound. Future research directions - both physiological and methodological - are outlined.

2. Background

Maintenance of adequate cerebral blood flow (CBF) is necessary for normal brain function and survival. That the brain receives ~15% of total cardiac output and is responsible for ~20% of the body's oxygen consumption, despite being 2-3% of total body weight, is testament to its high energetic cost. This, combined with a very limited ability to store energy (the brain's total energy pool would theoretically allow it to function for ~12 minutes were energy substrate supply abolished) requires effective regulation of blood supply. Numerous pathologies such as head trauma, carotid artery disease, subarachnoid haemorrhage and stroke result in disturbances to the regulatory mechanisms controlling CBF (Hossmann, 1994; Panerai, 2009). However, the skull makes it difficult to measure parameters such as blood flow and blood velocity. Many approaches such as radio-opaque tracers, radioactive markers and similar methods are inadequate because of poor temporal resolution (see See Table (appendix) for a summary of the advantages and disadvantages of other methods). Key factors that determine adequate CBF for maintenance of cerebral oxygen delivery are: (1) sensitivity to changes in arterial PO_2 and PCO_2 (cerebrovascular reactivity) and the unique ability to extract a large amount of

available oxygen; (2) effective cerebral autoregulation (CA) that assists maintenance of CBF over a wide range of perfusion pressures, helping to prevent over/under perfusion and consequent risk of hemorrhage or ischemia; and, (3) matching of local flow to localized metabolic needs (neurovascular coupling; NVC). The high temporal resolution and non-invasive nature of transcranial Doppler ultrasound (TCD) make it a useful tool in the assessment of integrative cerebrovascular function in terms of cerebral reactivity, autoregulation, and NVC. New technologies are further increasing the utility of TCD. For example, combining TCD with microbubble contrasting agents allow for quantification of local changes in perfusion for measuring absolute volumetric flow (Powers *et al.*, 2009). However, the interaction of ultrasound with microbubble contrast agents is complex and beyond the scope of this review; the reader is referred to (Powers *et al.*, 2009) for a detailed review of the current state of contrast TCD technology. With or without contrast, a TCD machine is relatively inexpensive ($20,000 to $50,000 USD); moreover, TCD is easy to use and it is safe in healthy and disease states alike. For these reasons TCD is practical in the clinical setting, where it is used to assess a variety of different cerebrovascular pathologies.

The principal aim of this chapter is to summarize the utilities of TCD in the assessment of cerebrovascular function with respect to other common measurement tools. Specifically, we aim to: (1) examine the advantages and disadvantages of TCD in the context of other imaging metrics; (2) highlight the optimum approaches for insonation of the basal intra-cerebral arteries; (3) provide a detailed summary of the utility of TCD for assessing cerebrovascular reactivity, autoregulation and neurovascular coupling and the clinical application of these measures; and (4) provide recommendations on the integrative assessment of cerebrovascular function and avenues for future research.

2.1 Techniques for the measurement of cerebral blood flow and velocity

Kety and Schmidt (1945) were the first to quantify CBF using an inert tracer (e.g., nitrous oxide, N_2O). The reference method for the measurement of global CBF, the Kety-Schmidt method is based on the Fick principle, whereby the arterio-venous difference of an inert tracer is proportional to the volume of blood flow through the brain (Kety & Schmidt, 1948). The tracer is infused until tension equilibrium is attained (the saturation phase) and then terminated, after which the concentration falls toward zero (the desaturation phase). Simultaneous arterio-jugular venous samples are withdrawn during either phase and CBF calculated by the Kety-Schmidt equation:

$$CBF = 100 \times \lambda \times \frac{C_{jv}(\text{equilibrium})}{\int_{t=0}^{t=\infty} (C_{jv}(t) \times dt) - \int_{t=0}^{t=\infty} (Ca(t) \times dt)},$$

where Cjv(t) and Ca(t) are the jugular-venous and arterial concentration, respectively, of the tracer at time t (in minutes), and λ is the brain-blood partition coefficient (in ml g^{-1}). The global cerebral metabolic rate (CMR) of substance *x* is given by the Fick principle as:

$$CMR = CBF \times a\text{-}jv\ D(x) = CBF \times (Ca(x) - Cv(x)),$$

where a-jv D (x) is the arterial to jugular-venous concentration of x. This provides a valid CMR due to the identical sampling sites (regions of interest) for the CBF measurement and the a-v D(x) (See Figure 1).

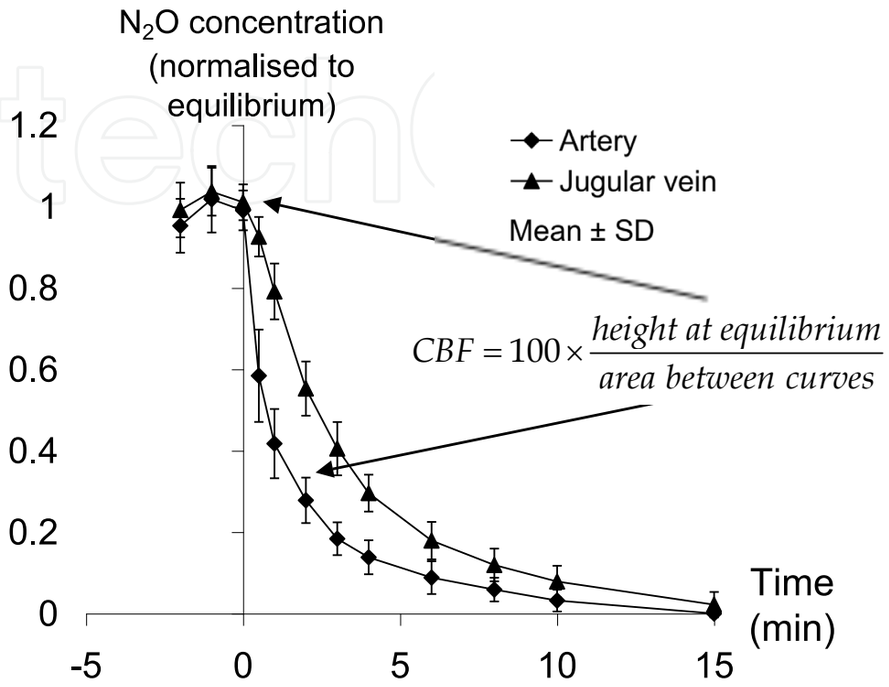

Fig. 1. The Kety-Schmidt method using N_2O. N_2O concentration is given on the y-axis as the percent of equilibrium concentration (mean ± SD) versus time, by discontinuous blood sampling in the desaturation phase during normocapnia.

Theoretically, this principle can be exploited using any freely diffusible tracer; indeed N_2O, ^{133}Xe, hydrogen, and iodoantipyrine have all been utilized (Edvinsson & Krause, 2002). While this method did stimulate seminal research in cerebrovascular physiology (Kety, 1999), there are several important limitations: measurements are taken over the course of minutes, making it impossible to assess dynamic changes in CBF; only a global, but not regional, measure of CBF, cerebral metabolic rate, or blood-brain substrate exchange is possible; internal jugular and peripheral arterial lines are necessary making it quite invasive; and, finally, the value of cerebral oxygen consumption must be assumed (Kety & Schmidt, 1948). Furthermore, venous outflow from the brain may not be symmetrical, with 50% of individuals exhibiting cortical drainage of venous blood mainly through the right internal jugular vein, and subcortical largely through the left. Two decades later, the measurement of cerebral oxygen consumption was improved using radioactive inert gases ^{85}Kr (Lassen *et al.*, 1963)] and ^{133}Xe (Harper & Glass, 1965) that allow extracranial imaging of gamma emission from the cerebral cortex. However, the aforementioned temporal resolution combined with potential problems of extra-cranial tissue sampling and inadequate desaturation are limitations that remain with these approaches.

The use of Doppler ultrasound was first described as early as 1959 for assessing blood velocity in the extracranial vessels (Miyazaki & Kato, 1965). The thickness of the skull bones greatly attenuates the penetration of ultrasonic waves making noninvasive use of the technique difficult. Ultrasound was therefore limited to surgical procedures, or to use in children with open fontanels. However, Aaslid *et al* (1982) demonstrated that the attenuation of sound by bone within the frequency range of 1-2MHz was far less than conventional frequencies of 3-12MHz. Indeed, insonation is possible through thinner regions of the skull, termed "acoustic" windows, making it feasible to measure static and dynamic blood velocities within the major cerebral arteries. For the first time, a non-invasive measure of beat-to-beat changes in blood velocity in the vessels of the brain with superior temporal resolution than indicator-dilution techniques was available. However, it is imperative to note that TCD cannot measure CBF *per se*. Rather, TCD measures the *velocity* of red blood cells within the insonated vessel. Moreover, only the larger basal arteries provide an adequate signal for measurement of cerebral blood velocity with TCD. Because these arteries tend to deliver oxygenated blood to large regional areas of the brain, TCD gives an index of global, rather than local, stimulus-response. This is an important distinction given that local changes in CBF likely differ (Hendrikse *et al*., 2004; Nöth *et al*., 2008; Piechnik *et al*., 2008). Certainly, there is a notable dissimilarity in vasoreactivity across the cerebrovasculature. At least in hypercapnia, small vessels and capillaries possess much higher reactivity to CO_2 (Mandell *et al*., 2008), and vasculature residing within gray matter show higher reactivity than vasculature within white matter (Nöth *et al*., 2008; Piechnik *et al*., 2008). This lack of spatial resolution in brain hemodynamics is the principal limitation of TCD. There are a variety of modern imaging techniques that allow sufficient spatial resolution to discern localized brain perfusion [see See Table (appendix) for a summary and (Wintermark *et al*., 2005) for a detailed review].

3. The cerebrovascular exam

3.1 Recording principles

The principles of TCD are the same as extracranial Doppler ultrasound: the Doppler probe emits sound waves that are reflected off moving red blood cells, which are subsequently detected by the transducer. The resultant Doppler-shift is proportional to the velocity of the blood (DeWitt & Wechsler, 1988; Aaslid, 1986a). Duplex ultrasound (simultaneous two dimensional B-mode and pulse-wave velocity) typically used in vascular ultrasound to measure both vessel luminal diameter and blood velocity (and therefore volumetric flow; see Section VI) is not possible with current TCD systems due to lack of resolution. Because the diameter of the insonated vessel is unknown, TCD only measures cerebral blood velocity (CBV) *not* absolute volumetric flow. The velocity of blood through a vessel is proportional to the fourth power of vessel radius; the measurement of CBV by TCD assumes constant diameter of the insonated vessel – this assumption has been found to be valid in various studies (Serrador *et al*., 2000; Bishop *et al*., 1986; Nuttall *et al*., 1996; Peebles *et al*., 2008; ter Minassian *et al*., 1998; Valdueza *et al*., 1997). Despite these validations, however, it remains possible that the cerebral conduit vessels do, in fact, change diameter, and as such, any TCD data should be openly interpreted with this possibility in mind. In addition, other problems remain for meaningful velocity quantification. For example, the velocity of blood through a vessel – in the presence of laminar flow – is approximately parabolic in shape,

with the fastest velocity in the center of the vessel. The Doppler signal consequently represents not a single value but rather a distribution of velocities, therefore requiring mathematical manipulation to extract meaningful velocity values. Typically, a power spectrum distribution is produced from segments of ~5 seconds using a Fast Fourier transform, and maximum or mean velocity is calculated from the maximum or intensity weighted mean, respectively (see Figure 2; Lohmann *et al.*, 2006; Aaslid, 1986b).

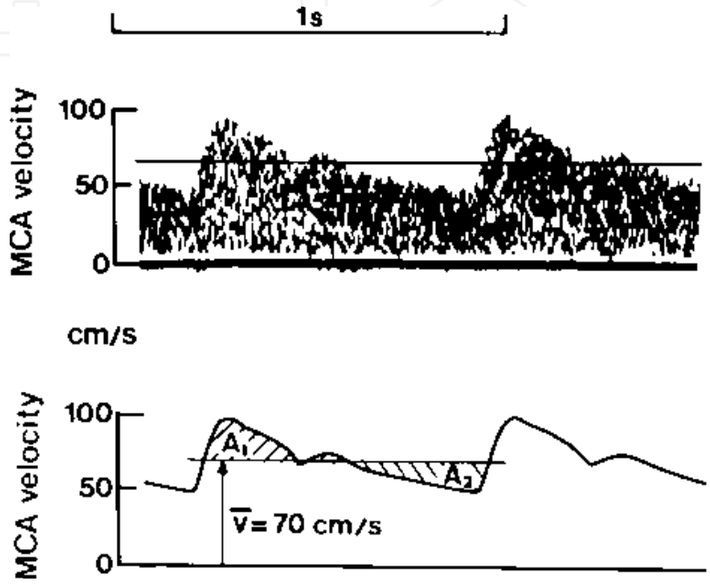

Fig. 2. (A) Spectral display of middle cerebral artery Doppler signal. (B) Maximal velocity outline of Doppler spectrum with the horizontal line representing the mean velocity and systolic and diastolic velocities above and below, respectively. Modified from Aaslid et al. J Neurosurg (1982) vol. 57 (6).

A frequency of 2MHz is typically used for TCD because higher frequencies do not sufficiently penetrate the bones of the skull (DeWitt & Wechsler, 1988; Aaslid *et al.*, 1982). Despite the increased penetration of TCD, an acoustic window in the skull is necessary for adequate insonation of intracerebral arteries. The choice of window, however, can dramatically affect the type of recording possible. For example, insonation through the transtemporal or foramen magnum windows allow use of a headpiece for securing the Doppler probe, whereas this is not possible when insonating through the optic canal.

Imaging modalities such as colour-coded Doppler and power Doppler, significantly increase the reliability of TCD as direct visualization of the target vessel facilitates better insonation angle correction (Martin *et al.*, 1995). Studies have demonstrated that the use of colour-coded and/or power TCD facilitates: (1) an improved signal-to-noise ratio with transcranial insonation (Postert *et al.*, 1997); (2) insonation in the presence of poor acoustic windows, particularly when combined with the use of contrast (Nabavi *et al.*, 1999; Gerriets *et al.*, 2000); (3) the measurement of arterial diameter threshold for collateral flow in the circle of Willis (Hoksbergen *et al.*, 2000); and, (4) an increase in the diagnostic sensitivity for cerebral vasospasm (Sloan *et al.*, 2004). Readers are referred to Willie et al., (2011b) for a detailed review of general TCD principles.

4. Regulation of cerebrovascular function

The cerebral vasculature rapidly adapts to changes in perfusion pressure (cerebral autoregulation; CA), regional metabolic requirements of the brain (neurovascular coupling), autonomic neural activity (Cassaglia *et al.*, 2009; Cassaglia *et al.*, 2008), and humoral factors (cerebrovascular reactivity). Regulation of CBF is highly controlled and involves a wide spectrum of regulatory mechanisms that together work to provide adequate oxygen and nutrient supply (Ainslie & Duffin, 2009; Ogoh & Ainslie, 2009a; Edvinsson & Krause, 2002; Panerai *et al.*, 1999a; Querido & Sheel, 2007); (Ainslie & Tzeng, 2010; Lucas *et al.*, 2010a). Indeed, the cerebral vasculature is highly sensitive to changes in arterial blood gases, in particular the partial pressure of arterial carbon dioxide ($PaCO_2$) (Ainslie & Duffin, 2009). It is thought that CA acts to change cerebral vascular resistance via vasomotor effectors, principally at the level of the cerebral arterioles and pial vessels (Edvinsson & Krause, 2002). Additionally, neuronal metabolism elicits an effect on CBF as necessitated by changes to regional oxygen consumption, with the sympathetic nervous system possibly playing a protective role in preventing over-perfusion in the cerebral vasculature ((Ainslie & Tzeng, 2010; Tzeng *et al.*, 2010a; Tzeng *et al.*, 2010b; Tzeng *et al.*, 2010c; Wilson *et al.*, 2010; Cassaglia *et al.*, 2009; Cassaglia *et al.*, 2008).

4.1 Regulation by arterial PCO_2

The cerebral vasculature is highly sensitive to changes in arterial blood gas pressures, in particular $PaCO_2$, which exerts a pronounced effect on CBF. Alveolar ventilation, by virtue of its direct effect on $PaCO_2$, is consequently tightly coupled to CBF. The response of CBF to $PaCO_2$ is of vital homeostatic importance as it directly influences central CO_2/pH, which is the central chemoreceptor stimulus (Chapman *et al.*, 1979). In response to increases in $PaCO_2$, vasodilation of downstream arterioles increases CBF. This, in turn, lowers $PaCO_2$ by increasing tissue washout, resulting in vessel constriction, and a subsequent decrease in CBF. Functional modulation of CBF by $PaCO_2$ influences pH at the level of the central chemoreceptors and directly implicates CBF in the central drive to breath (reviewed by Ainslie & Duffin, 2009; also see (Fan *et al.*, 2010a; Fan *et al.*, 2010b; Lucas *et al.*, 2010b). Indeed, previous studies have found a correlative link between blunted cerebrovascular CO_2 reactivity and the occurrence of central sleep apnea in patients with congestive heart failure (Xie *et al.*, 2005), and also in the pathophysiology of obstructive sleep apnea (Burgess *et al.*, 2010; Reichmuth *et al.*, 2009).

4.2 Regulation by arterial PO_2

Hypoxia is a cerebral vasodilator as reflected by a proportional increase in CBF with decreasing PaO_2 in conditions of isocapnia (Reviewed in (Ainslie & Ogoh, 2010). However, the resultant hyperventilation that accompanies hypoxic exposure yields hypocapnia that induces a counteracting cerebral vasoconstriction and decreased CBF. Indeed, a threshold of <40mmHg PO_2 is required in the face of prevailing hypocapnia for cerebral vasodilation to occur (Ainslie & Ogoh, 2010). This minor sensitivity is clinically relevant given the arterial hypoxemia encountered during exercise in elite athletes (Ogoh & Ainslie, 2009a; Ogoh & Ainslie, 2009b) and at high altitude (Ainslie & Ogoh, 2010) as well as in certain pathologies such as chronic lung disease and heart failure (reviewed in Ainslie & Ogoh, 2010 and Ainslie

& Duffin, 2009; See also: (Galvin *et al.*, 2010). The extent to which changes in cerebrovascular reactivity to hypoxia are related to pathological outcome is unknown. Moreover, unlike the CO_2 reactivity test, complex feedback (Kolb *et al.*, 2004; Ito *et al.*, 2008; Robbins *et al.*, 1982) or feed-forward (Slessarev *et al.*, 2007) gas manipulation techniques are needed to independently control $PaCO_2$ and PaO_2.

4.3 Neuronal metabolism and coupling

The effect of neural activity on CBF was demonstrated approximately 130 years ago in patients with skull defects (Mosso, 1880). Neurovascular coupling can be utilized as a sensitive method to test the function of cerebral vasculature. This activation–flow coupling describes a mechanism that adapts local CBF in accordance with the underlying neuronal activity (Girouard & Iadecola, 2006). The adaptation of regional CBF is based on local vasodilation evoked by neuronal activation, but the cellular mechanisms underlying neurovascular coupling are not fully understood. Synaptic activity has been shown to trigger an increase in the intracellular calcium concentration of adjacent astrocytes, which can lead to secretion of vasodilatory substances – such as epoxyeicosatrienoic acid, adenosine, nitric oxide, and cyclooxygenase-2 metabolites – from perivascular end-feet, resulting in increased local CBF (reviewed by Jakovcevic & Harder, 2007). Thus, astrocytes, via release of vasoactive molecules, may mediate the neuron-astrocyte-endothelial signaling pathway and play a profound role in coupling blood flow to neuronal activity (reviewed by (Iadecola & Nedergaard, 2007). Indeed, the 10-20% increase in CBF observed during aerobic exercise is likely due to combined elevations in cortical neuronal activity in addition to elevations in mean arterial pressure (MAP) and $PaCO_2$ (reviewed by (Ogoh & Ainslie, 2009a). Yet, even during exercise neurometabolic coupling with visual stimulation remains intact (Willie *et al.*, 2011a). The relative contribution of neurometabolic factors (i.e., neurovascular coupling) and systemic factors (i.e., increased $PaCO_2$ and blood pressure) is currently unknown.

4.4 Cerebral autoregulation

CBF is traditionally thought to remain relatively constant within a large range of blood pressures (60 to 150 mm Hg), at least in non-pathological situations (Lassen, 1959). This unique characteristic of the mammalian brain is known as cerebral autoregulation (CA). If CA fails, the brain is at risk of ischemic damage at low blood pressures or hemorrhage at high blood pressure. Preceding the advent of technologies with temporal resolution capable of measuring changes in CBF over the course of seconds, CA was measured under steady-state conditions (*See Section 2.1*). This "static" CA is a measure of cerebrovascular regulation of gradual changes in perfusion pressure. Traditionally, static CA was believed to hold CBF constant through a MAP range of ~60-150 mmHg (Lassen, 1959), but this concept has been recently challenged with evidence to support CBF closely paralleling changes in blood pressure (Lucas *et al.*, 2010a). Furthermore, static CA through this supposed autoregulatory range is difficult to assess because the upper range of blood pressures can only be achieved in healthy individuals using relatively high-dose pharmacological intervention. Indeed, we and others, have found that induction of hypertension using continuous phenylephrine infusion produces cardiotoxic effects on ECG, limiting MAP increases to <120 mmHg. Moreover, pharmacologically induced changes in BP also cause marked changes in

ventilation; thus, the confounding influence of arterial PCO_2 needs to be considered. The extent to which a normal healthy human can cope with extreme static changes in BP is unknown for obvious reasons. Regardless, even within the "autoregulatory range", static autoregulation appears to be influenced by blood pressure (Immink *et al.*, 2008; Lucas *et al.*, 2010a).

Dynamic CA (*d*CA) describes the ability of the cerebral vasculature to resist *acute* changes in perfusion pressure, (due to changes in arterial blood pressure) over a short time-course of less than five seconds (Zhang *et al.*, 1998). *d*CA can be quantified from either spontaneous fluctuations in MAP, or from stimulus-induced changes in MAP. With increased utilization of TCD a number of methods of MAP perturbation and *d*CA quantification have been developed.

That CBF appears to vary directly with MAP, suggests that arterial baroreflex regulation of peripheral blood pressure likely plays a more significant role in CBF control than previously thought (Lucas *et al.* (2010a). Moreover, Tzeng *et al* (2010a) showed an inverse relationship between cardiac baroreflex sensitivity and *d*CA, suggesting the presence of compensatory interactions between peripheral blood pressure and central CBF control mechanisms, directed to optimizing CBF control. Such interactions may account for the divergent changes in CA and baroreflex sensitivity seen with normal aging, and in clinical conditions such as spontaneous hypertension (Serrador *et al.*, 2005), autonomic failure (Hetzel *et al.*, 2003), and chronic hypotension (Duschek *et al.*, 2009). Some evidence also suggests that free radicals – particularly superoxide anion observed in pathologies such as ischemic and traumatic brain injury – causes impaired CA and increased basal CBF through activation of potassium channels within vascular smooth muscle cells (Zagorac *et al.*, 2005).

5. Assessment of cerebrovascular function

In this section we provide a practical overview of methods used to assess cerebral autoregulation (CA) including the use of suprasystolic thigh cuff, postural alterations, lower body negative or oscillatory pressure, the Valsalva maneuver, the Oxford technique and transfer function analysis.

5.1 Suprasystolic thigh cuffs

The rapid release of thigh cuffs inflated to suprasystolic pressures for ≥2 minutes elicits a transient hypotension (Aaslid *et al.*, 1989; Mahony *et al.*, 2000; Tiecks *et al.*, 1995a). The rate of regulation (RoR), quantifies the rate at which cerebrovascular resistance (CVR), or conductance changes in response to a perturbation in MAP and can be given by Equation 1:

$$\text{RoR} = (\Delta\text{CVR}/\Delta t)/\Delta\text{MAP}$$

where ΔCVR is given by $\text{MCAv}_{\text{mean}}/\text{MAP}$, and ΔMAP by control $\text{MAP-MAP}_{\text{mean}}$. Δ*t* is taken as the 2.5 second period one second following thigh cuff release (Figure 3).

This time interval was originally put forth by Aaslid *et al* (Aaslid *et al.*, 1989) based on two factors: (1) the change in CVR is relatively linear during this period, allowing a slope of the response to be taken; and, (2) it was thought that the latency of the baroreflex response was such that within the first 3.5 seconds of the cerebrovascular response to a hypotensive

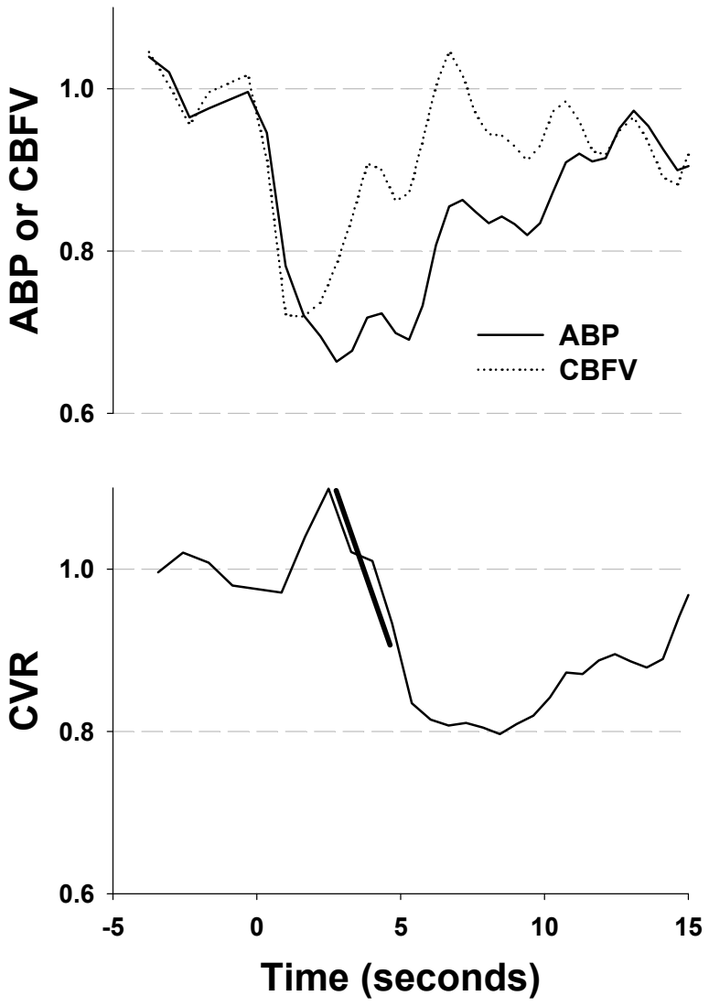

Fig. 3. Typical changes in arterial blood pressure (ABP), cerebral blood flow-velocity (CBFV) and cerebrovascular reactivity (CVR) in response to thigh cuff deflation, for determining dynamic cerebral autoregulation (CA). All tracings are shown in normalized units relative to control pre-release values from -4 to 0 seconds. Straight line (bold line) through CVR (bottom figure) curve is determined by regression analysis of data obtained in the interval from 1 to 3.5 seconds after thigh cuff release and is used for calculating rate of regulation (RoR).

challenge, only cerebrovascular mechanisms (i.e., *d*CA) would be involved in regulation of CBF. However, the drop in arterial pressure following thigh cuff deflation engages the arterial baroreflex within 0.44 seconds of baroreceptor unloading by neck pressure (Eckberg, 1980) causing transient tachycardia. Although unilateral thigh cuff deflation was reported to not alter central venous pressure (Fadel *et al.*, 2001), unpublished observations from our laboratory indicate this may not be the case for bilateral thigh-cuff release. It is unclear, consequently, how cardiac output is affected following bilateral thigh-cuff release. Some authors (Ogoh *et al.*, 2003; Ogoh *et al.*, 2007), but not all (Deegan *et al.*, 2010), have reported

that increases in cardiac output can augment CBF; thus, it is plausible that baroreflex function may exert a modulating influence on dynamic CBF regulation such that RoR reflects the integrated response of both the baroreflex and *d*CA (Ogoh *et al.*, 2009). The thigh cuff technique is also somewhat painful, with inflation often associated with an increase in MAP that is maintained until cuff release. The influence of sympathetic nervous system activity in response to discomfort is not known, but a minimum 8-minute recovery period has been recommended following cuff deflation (Mahony *et al.*, 2000).

Another prevalent method to quantify the *d*CA response to thigh cuff release, termed the autoregulatory index, was proffered by Tiecks *et al* (1995a). This approach uses a second order differential equation to relate changes in MAP and three predefined model parameters (T: time constant; D: damping factor; and *k*: autoregulatory gain) to generate ten templates of CBV-response to a non-pharmacologically induced transient hypotension (Figure 4). Typically, rapid thigh-cuff deflation is used to induce a transient hypotension. According to the Tiecks model, the autoregulatory index assigns an integer value to each of ten template curves (0-9). These coefficients are generated using a second-order linear differential equation:

$$dP_n = \frac{\text{MAP - MAP}_{\text{base}}}{\text{MAP}_{\text{base}} - \text{CCP}}$$

$$x2_n = x2_{n-1} + \frac{\left(x1_n - 2D \cdot x2_{n-1}\right)}{f \cdot T}$$

$$x1_n = x1_{n-1} + \frac{\left(dP_n - x2_{n-1}\right)}{f \cdot T}$$

$$mV_n = \text{MCAv}_{\text{base}} \cdot \left(1 + dP_n - k \cdot x2_n\right)$$

where dP_n is the normalized change in mean arterial blood pressure (MAP) relative to baseline MAP (MAP_{base}) and adjusted for estimated critical closing pressure (CCP); $x2_n$ and

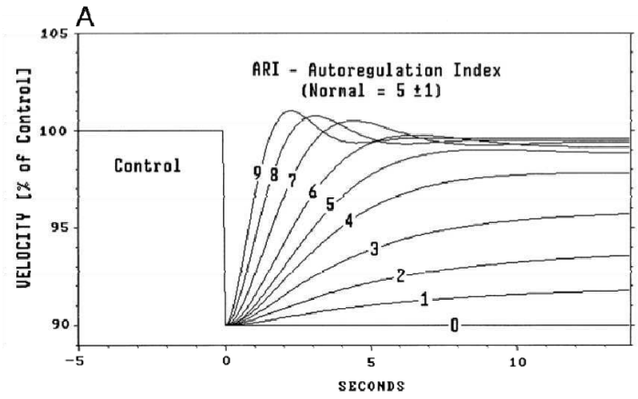

B

T, s	D	K	ARI	dROR, %/s
...	0.00	0	0	0 (No autoregulation)
2.00	1.60	0.20	1	2.5
2.00	1.50	0.40	2	5.0
2.00	1.15	0.60	3	10.0
2.00	0.90	0.80	4	15.0
1.90	0.75	0.90	5	20.0 ("Normal" autoregulation)
1.60	0.65	0.94	6	30.0
1.20	0.55	0.96	7	40.0
0.87	0.52	0.97	8	60.0
0.65	0.50	0.98	9	80.0 (Fastest autoregulation)

Fig. 4. (A) Responses of CA model (ARI) to step changes in blood pressure. The CBFV response curve model with 10 different degrees of dynamic CA is calculated by this method. 9 is the highest degree of dynamic CA. (B) Tabular comparison of ARI, and associated constants, with percentage RoR; T indicates time constant; D, damping factor; K, autoregulatory dynamic gain; ARI, autoregulation index; and dROR, dynamic rate of regulation.

$x1_n$ are state variables (equal to 0 at baseline); mV_n is modeled mean velocity; $MCAv_{base}$ is baseline $MCAv_{mean}$; f is the sampling frequency, and n is the sample number. The mV_n generated from ten predefined combinations of parameters T (time constant), D (dampening factor) and k (autoregulatory gain) that best fit the actual $MCAv_{mean}$ recording is taken as an index of dynamic CA. A value of 0 represents no autoregulation where CBV passively follows perfusion pressure, and a value of 9 represents perfect CA where changes in perfusion pressure produce no alteration to CBV. The autoregulatory index has also been derived from spontaneously occurring blood pressure and cerebral blood vessel velocity fluctuations using transfer function analysis (Panerai *et al.*, 1999a; Panerai *et al.*, 2001). However, the validity of comparison between a linear model and that from a transient hypotensive stimulus may be questionable (see *Transfer function analysis* below).

5.2 Postural alterations

Because of the confounders inherent to both pharmacological and non-physiological methods of BP alteration (e.g., thigh-cuff release) postural maneuvers to alter blood pressure have been utilized for CA assessment. The simple act of standing from a sitting, supine, or squat position is enough to elicit a transient drop in BP of ~35 mmHg and associated drop in CBV (Thomas *et al.*, 2009; Murrell *et al.*, 2009; Murrell *et al.*, 2007). RoR (Sorond *et al.*, 2005), ARI, and transfer function analysis (Claassen *et al.*, 2009) have all been used to quantify the *d*CA response to postural changes in BP.

5.3 Valsalva maneuver

Forced expiration against a closed glottis regularly occurs during normal daily activities such as during defecation and lifting. The Valsalva maneuver has been well described in the literature (Smith *et al.*, 1996; Tiecks *et al.*, 1996) and consists of four phases: (1) increased MAP due to increased intrathoracic pressure; (2a) impaired atrial filling and resultant drop in MAP, followed by; (2b) a baroreceptor mediated tachycardia and increase in MAP; (3) release of strain and drop in intrathoracic pressure which decreases MAP; and (4) baroreceptor mediated sympathetic activity that drives MAP above baseline in the face of transient hypotension. Due to impaired atrial filling, combined with raised intracranial pressure induced by increased intrathoracic pressure during strain, there is a marked decrease in cerebral perfusion pressure during the onset of phase 2a. This drop in perfusion pressure provides an adequate stimulus for measurement of *d*CA (Tiecks *et al.*, 1996; Tiecks *et al.*, 1995b; Zhang *et al.*, 2002). The Valsalva maneuver may, however, be confounded by its inherent physiological complexity. Changes in $PaCO_2$ are likely to occur over the course of the breath-hold, and although it has been suggested that there is sufficient time delay between changes in end-tidal PCO_2 ($PetCO_2$) and subsequent changes in CBF to preclude the breath-hold from effecting measured values of CA, this is not known for certain (Hetzel *et al.*, 2003). Furthermore, changes in intrathoracic pressure likely vary between individuals, and throughout the maneuver there are changes in intracranial pressure, venous outflow pressure and resistance. And though there is a period of relatively stable intracranial pressure, the possibility of these changes confounding measures of CA certainly exist. Nonetheless, Tiecks *et al* (1996) described the Valsalva ARI as the ratio between the relative changes in cerebral blood flow velocities and blood pressure, calculated as:

$$ARI_{Valsalva} = ((CBFV(iv)/CBFV(i)/(BP(iv)/BP(i))$$

where I and IV signify phases one and four of the Valsalva response, respectively. CBF is modified proportionally more than BP, implying that autoregulation is preserved, if the ratio is found to be >1. Because minor variations in expiratory pressure results in changes in the various stages of the maneuver, it is imperative to standardize the technique between and within subjects.

5.4 Transfer function analysis

Transfer function analysis (TFA) for the assessment of dynamic CA is based on analysis of the coherence, frequency and phase components of spontaneous changes in MAP, and the resultant degree to which these changes are reflected in CBV (Zhang *et al.*, 1998). It is thought that CA acts as a high pass-filter, effectively dampening low-frequency oscillations (<0.07Hz) (Panerai *et al.*, 1998; Zhang *et al.*, 1998). An advantage to this method is the ability to complete the measurement in a subject at baseline without the need for any pharmacological or physiological manipulation of BP. However, the corollary is that TFA cannot be used to analyze the CA response to a transient and directional change in BP (i.e., it cannot distinguish between "upward" and "downward" fluctuations in BP). Furthermore, TFA assumes that the dynamic autoregulatory responses to spontaneous fluctuations in BP are linear. This is to say that TFA assumes CA is equally effective in attenuating changes in cerebral perfusion in response to both hyper and hypotensive changes in MAP; however, this may not be the case (Aaslid *et al.*, 2007; Tzeng *et al.*, 2010b). If hysteresis is a natural characteristic of CA (i.e., differential CA depending on directionality of the blood pressure change), than the assumptions of linear techniques such as TFA may not be valid. An extension of TFA is impulse response analysis, whereby spontaneous changes in MAP are inversely transformed back to the time domain (Panerai, 2008). In other words, the impulse response function is an inverse algorithm of the Fast Fourier analysis of frequency shifts of blood velocity, as a time domain function. This allows time-domain models such as the ARI to be applied to spontaneous data (Czosnyka *et al.*, 2009). Again, if the CA response is not linear, comparison of ARI's generated from linear models, to those generated from a transient hypotensive or hypertensive stimulus, may also not be valid. A limitation of CA assessment using spontaneous data is the small magnitude and inconsistency of spontaneous pressure oscillations (Taylor *et al.*, 1998).See Table (appendix).

5.5 The Oxford technique

The Oxford technique is the method of using vasoactive drug injections (most often phenylephrine hydrochloride and sodium nitroprusside; the modified Oxford technique) to provoke baroreflex responses, and has been widely used since (Smyth *et al.*, 1969) utilized bolus angiotensin injected intravenously during wakefulness and sleep; the R-R interval response to changes in arterial BP provides an index of cardiac baroreflex sensitivity. Despite its prevalence in baroreflex research until recently, the technique had not been utilized for assessment of CA, despite providing some distinct advantages in CA quantification. Blood pressure can be raised or lowered, allowing both positive and negative CA gains to be assessed independently – an important consideration given

evidence that CA may be more effective at dealing with increases in blood pressure than decreases in blood pressure (Aaslid *et al.*, 2007; Tzeng *et al.*, 2010b). The Oxford technique is also largely painless, reducing the influence of pain induced sympathetic activity. *d*CA is quantified by taking the slope of the linear regression between CBV and MAP – the slope is inversely proportional to the efficacy of cerebral autoregulation in maintaining CBV. This is to say, a slope of zero would imply perfect autoregulation where CBF remains constant across the entire range of MAP, while a gain equal to 1 would reflect the total absence of autoregulation (Tzeng *et al.*, 2010b). The limitations inherent to any pharmacological approach remain manifest with this technique, and although there is supportive evidence (Greenfield & Tindall, 1968) the assumption that there is no direct drug-effect on the cerebral vasculature has been questioned (Brassard *et al.*, 2010). However, direct effects of PE and SNP on cerebral vasculature are considered unlikely given that the blood-brain barrier normally prevents endogenous circulating catecholamine from binding to α_1-adrenoreceptors in small cerebral vessels (Ainslie & Tzeng, 2010; MacKenzie *et al.*, 1976; McCalden *et al.*, 1977).

5.6 Oscillating blood pressure

A criticism of TFA is that it analyses relatively small natural swings in blood pressure. Coherence between pressure and CBF is often low (<0.5) making it difficult to ascertain the statistical and TFA model reliability, as well as the causal relationship between these variables. These difficulties have been partially overcome by inducing large-amplitude blood pressure oscillations through either repeated squat-standing or oscillatory lower body negative pressure at frequencies associated with CA (Claassen *et al.*, 2009; Hamner *et al.*, 2004). See Figure 5 for detailed explication of this technique.

5.7 Cerebrovascular reactivity

Cerebrovascular reactivity gives an index of reactivity of the intracranial vessels in response to a stimulus – typically either pharmaceutical (e.g., acetazolamide) or through ventilatory alterations of $PaCO_2$. There is differential reactivity to CO_2 across the cerebral vasculature. Cerebrovascular CO_2 reactivity assessed by TCD gives a global measure of reactivity compared to more sophisticated techniques such as pulsed arterial spin labeling MRI and positron emission tomography that both allow a specific brain area to be assessed. Typically, a hypercapnic stimulus is utilized to assess reactivity, and using TCD to assess CBV reactivity can be given by:

$$CA = \Delta CBV(\Delta PetCO_2)^{-1}$$

Similarly, volitional hyperventilation can be utilized decrease $PetCO_2$, such that reactivity to hypo and hypercapnia can be assessed. From a clinical perspective, impairment of cerebrovascular reactivity to CO_2 – as assessed by TCD – has been linked to such pathologies as obstructive and central sleep apnea (Burgess *et al.*, 2010; Reichmuth *et al.*, 2009), carotid artery stenosis (Widder *et al.*, 1994), hypertension (Serrador *et al.*, 2005), congestive heart failure (Xie *et al.*, 2005), and cerebral ischemic events (Wijnhoud *et al.*, 2006). It is also an established independent predictor of ischemic stroke (Markus & Cullinane, 2001; Silvestrini *et al.*, 2000; Vernieri *et al.*, 2001).

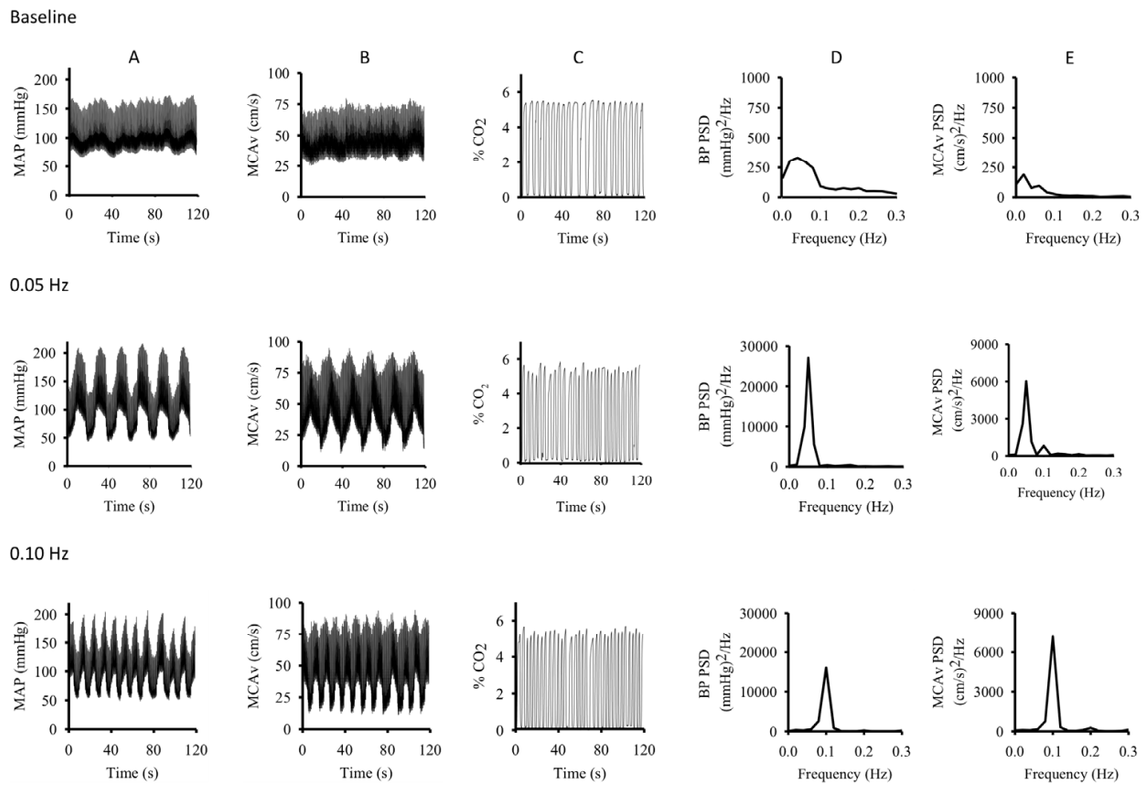

Fig. 5. Effects of repeated squat-stand maneuvers on (**A**) mean arterial blood pressure (Finapres; MAP), (**B**) middle cerebral artery blood velocity (Transcranial Doppler; MCAv), and (**C**) end-tidal CO_2. Raw waveforms are shown from a representative individual at rest (baseline, top row) and during repeated squat-stand maneuvers at 0.05 Hz (5-s squat, 5-s stand; middle row), and 0.1 Hz (10-s squat, 10-s stand; bottom row). A total of 600 s is displayed at rest and at 0.1 and 0.05 Hz; over the 120 s, 6 and 12 full cycles of the 0.05 and 0.1 Hz maneuvers occur, respectively. Note: 1) the large and coherent oscillations in MAP and MCAv during these maneuvers relative to resting conditions; 2) despite the strong hemodynamic effects, there is no distortion of MCAv and MAP waveforms; 3) end-tidal PCO_2 is well maintained; 4) the influence of 'targeting' 0.05Hz and 0.01Hz frequency ranges on blood pressure (BP) and MCAv power spectral densities (panels (**D**) and (**E**) respectfully). For example, the repeated squat-stand maneuvers at 0.05 results in a 40-fold increases in BP spectral power (compared with spontaneous VLF oscillations), while at 0.1 Hz, a 100-fold increase occurs relative to spontaneous LF oscillations. These augmented oscillations in BP led to 20-, and 100-fold increases in MCAv spectral power at 0.05, and 0.1 Hz, respectively. Thus increases in MCAv oscillations are relatively smaller than increases in BP oscillations at 0.05 Hz but not at 0.1 Hz, indicating more effective damping at the lower frequencies. Importantly, the coherence between BP and MCAv is typically much higher for repeated squat-stand maneuvers than for spontaneous oscillations (e.g., range (n=8): 0.6 to 0.99 vs 0.2 to 0.6, respectively). Thus, large oscillations in BP and MCAv induced during repeated squat-stand maneuvers not only provided strong and physiologically relevant hemodynamic perturbations, but also led to improved estimation of transfer function to assess dynamic cerebral autoregulation at the very low and low frequencies.

Acetazolamide can also be used to assess cerebrovascular reactivity. Acetazolamide inhibits carbonic anhydrase, the enzyme responsible for reversible catalyzation of H_2CO_3 formation from CO_2 + H_2O. Consequently it increases tissue PCO_2, leads to metabolic acidosis, and increased CBF. Although the exact mechanisms of acetazolamide-induced increases in CBF are not fully understood they likely involve both metabolic factors and direct as well as indirect vascular effects (Pickkers *et al.*, 2001); and reviewed by Settakis *et al.*, 2003). The use of acetazolamide for cerebrovascular reactivity assessment necessitates intravenous administration. However, in this form the drug can be costly, and depending on the country, difficult to procure. Regardless, confounds associated with cerebrovascular reactivity quantification using acetazolamide are not well understood, but it may directly effect the cerebral vasculature and can indirectly drive increased ventilation, which when combined with the need for intravenous administration and high-cost, makes acetazolamide less utilized than alteration of inspired CO_2. Regardless of the stimulus used, when assessing cerebrovascular reactivity, an absolute measurement of CBV is not as important as resolution of beat-to-beat changes in CBF from a pre-stimulus baseline.

5.8 Neurovascular coupling

Functional hyperemia describes the increased CBF to active areas of the brain where the demand for both nutrient delivery, and clearance of metabolic by-products is increased. The functional anatomy of the brain allows this neurovascular coupling to be easily and reliably examined by measurement of the sensorimotor or cognitive stimulatory effects on CBV – a method termed functional TCD (fTCD; Figure 6). This technique was first utilized by Aaslid *et al* (1987) who showed that blood velocity in the PCA changed with visual stimulation (see Hubel & Wiesel, 2005 for a comprehensive report of visual system physiology), but there are numerous studies in the neuro-cognitive literature that demonstrate consistent CBF changes in response to cognitive, verbal, and motor tasks (Rosengarten *et al.*, 2003; Aaslid, 1987; Deppe *et al.*, 2004; Klingelhöfer *et al.*, 1997; Silvestrini *et al.*, 1993; Stroobant & Vingerhoets, 2000).

Despite the poor spatial resolution inherent to TCD, many studies have examined the relationship between cognitive activation and CBF. For example, chronic hypotension depresses cognitive activity (Jegede *et al.*, 2009; Duschek *et al.*, 2008; Duschek & Schandry, 2007). Conversely, cognitive activity can be improved with pharmacological treatment of hypotension (Duschek *et al.*, 2007). These studies demonstrate that cognitive activity is positively related to neural tissue oxygen delivery, but the scope of fTCD is very broad. Studies have examined the effect of pharmacological agents (Rosengarten *et al.*, 2002a), Type I diabetes (Rosengarten *et al.*, 2002b), Alzheimer's disease (Rosengarten *et al.*, 2007), voluntary movements (Orlandi & Murri, 1996; Sitzer *et al.*, 1994), hemispheric language lateralization (Knecht *et al.*, 1998b; Dorst *et al.*, 2008; Markus & Boland, 1992; Knecht *et al.*, 1998a; Knecht *et al.*, 1998b), emotional processing (Troisi *et al.*, 1999), and attentional processes (Schnittger *et al.*, 1996; Schnittger *et al.*, 1997; Helton *et al.*, 2007; Knecht *et al.*, 1997) on neurovascular coupling. It has also been well characterized in clinical populations (Silvestrini *et al.*, 1993; Silvestrini *et al.*, 1995; Silvestrini *et al.*, 1998; Silvestrini *et al.*, 2000; Thie *et al.*, 1992; Njemanze, 1991; Bruneau *et al.*, 1992), and may be a useful paradigm for the evaluation of cerebrovascular function in certain disease states (Boms *et al.*, 2010).

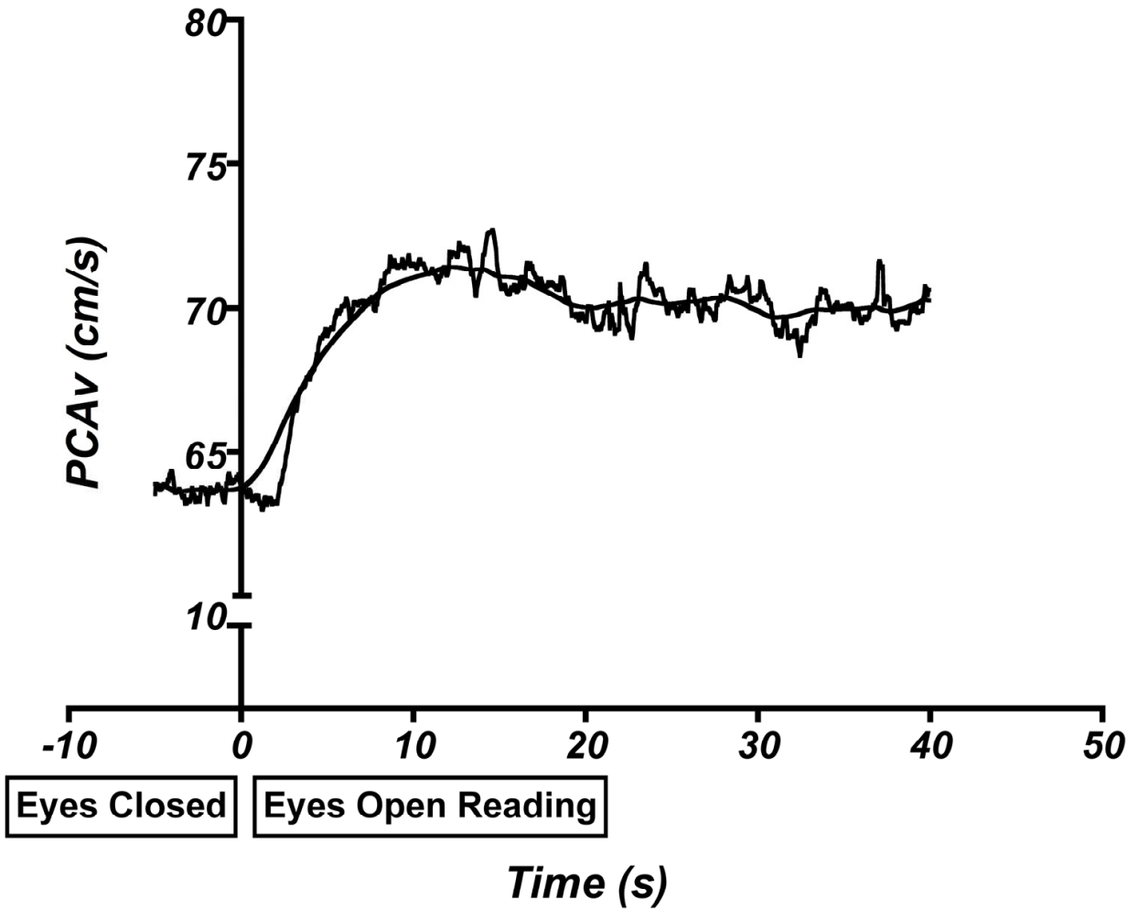

Fig. 6. Mean time course of peak systolic PCAv during visual stimulation (reading) while at upright-seated rest in 10 healthy young volunteers. Smooth line generated by locally weighted polynomial regression.

5.9 Estimation of intracranial and critical closing pressure using TCD

The critical closing pressure is the theoretical pressure at which blood flow within the cerebral vessels drops to zero, due to failure of the transmural pressure across a vessel to counteract the tension created by the vessel's smooth muscle. Measures of cerebrovascular resistance or compliance assume proportional linearity between blood flow and pressure, and that flow through a vessel ceases when the pressure is zero. Aaslid et al. (Aaslid *et al.*, 2003) demonstrated in humans that flow stops due to vessel collapse when perfusion pressure remains positive, making CCP a potentially better measure of cerebrovascular tone. CCP can be estimated by extrapolation of the CBV – blood pressure relationship to the pressure at which zero flow would theoretically occur. However, regardless of whether the entire pressure and velocity waveforms are used (Aaslid *et al.*, 2003), or the systolic and diastolic values only (Ogoh *et al.*, 2010), this technique typically yields an underestimate of CCP. Indeed, in some individuals the estimated CCP may even be negative, which is difficult to interpret physiologically. Furthermore, most studies have used peripheral blood pressure recordings that do not take into account pulse wave amplification in the periphery,

which further contaminate CCP estimation. The reader is referred to (Panerai, 2003) for a detailed review of the concept.

6. Clinical applicability of TCD

The low cost, excellent temporal resolution, and bedside availability of TCD make it an ideal tool for clinical diagnosis of acute and chronic cerebrovascular diseases. The principle area of clinical application of TCD is the assessment of pathologies that alter blood velocity within the intracranial arteries or veins. We particularly focus on vasospasm, stenosis, intracranial occlusions, thrombosis, critical closing pressure, brain death, and patent foramen ovale.

6.1 Vasospasm

Vasospasm is observed as a complication of subarachnoid hemorrhage with an incidence ranging between 30% and 70% depending if the vasospasm is symptomatic or angiographic, respectively. Because blood velocity within a vessel is inversely proportional to its cross-sectional area, the primary pathological condition that affects flow-velocity is vasospasm, which is therefore detectable with TCD (Aaslid *et al.*, 1982). Vasospasm can remain asymptomatic, but the factors leading to symptom presentation are largely unknown. Although diagnosis of vasospasm requires the presence of hyperaemia in addition to increased blood flow velocities (see the Lindegaard index, below), at least within the MCA, threshold values of MCAv are fairly well accepted. Velocities between 120 and 200 cm/s are indicative of a reduction in lumen diameter between 25% and 50%, and serious vasospasm and lumen diameter reduction greater than 50% is indicated with velocities above 200 cm/s (Tsivgoulis *et al.*, 2009). Hyperaemia must also be present to diagnose vasospasm; the Lindegaard Index is a ratio between the mean flow velocity in the MCA and that in the ICA, where values greater than 6 indicate severe vasospasm, between 3 and 6 indicate moderate vasospasm, and less than 3, hyperaemia (Rasulo *et al.*, 2008). The disadvantage of using the Lindegaard ratio is that it assumes a dichotomous condition – where there is either vasospasm or not – which may be misleading in certain patients. A promising diagnostic criterion is the use of a daily increase in the systolic pressure of more than 50 cm/sec; this avoids dichotomous classification of vasospasm, informs about the physiopathological trend towards vasospasm, thereby allowing the early identification of patients at risk. To further increase the accuracy of transcranial Doppler in the identification of cerebral vasospasm, thresholds in mean velocities of more than 160 cm/sec have accurately diagnosed cerebral vasospasm (Mascia *et al.*, 2003).

6.2 Stenosis

Typically TCD does not provide sufficient data for accurate identification of stenosis of a cerebral vessel, particularly in the posterior vessels that are more tortuous and have greater anatomic variability. Diagnosis of stenosis using TCD requires: (1) acceleration of flow velocity through the stenotic segment, 2) decrease in velocity below the stenotic segment, (3) bilateral asymmetry in flow, and (4) disturbances in flow (i.e., turbulence and murmurs) (Rasulo *et al.*, 2008). Diagnosis of stenosis using TCD has greater sensitivity and specificity in the anterior than in the posterior circulation due to the lower anatomic variability and relative ease of insonation of the anterior vessels.

6.3 Intracranial occlusion

TCD has excellent utility in diagnosis of occlusion within the cerebral vessels with sensitivity and specificity over 90% – particularly in patients where cerebral ischemia is present (Camerlingo *et al.*, 1993). Diagnosis is through absence or a profound reduction of flow at the normal position and depth, and/or consequent lack of signal for the vessels in the immediate vicinity of the occluded region. Furthermore, due to its non-invasiveness, TCD can easily be used to track the progression of an occlusion both before and after treatment (Rasulo *et al.*, 2008). Furthermore, recent data suggest an independent effect of the ultrasound in augmenting the thrombolysis of the occlusion in patients with acute MCA thrombosis (Eggers *et al.*, 2003; Eggers *et al.*, 2009). The Clotbust trial (Alexandrov *et al.*, 2004) demonstrated that the presence of residual flow signal, dampened waveform, and microembolic signals prior to thrombolysis was associated with increased likelihood of complete recanalisation after thrombolysis. Furthermore, in patients with acute ischemic stroke, continuous TCD significantly increased tissue plasminogen activator-induced arterial recanalization (Alexandrov, 2009). See (Alexandrov, 2006) for a review of the use of TCD in thrombolytic treatment of stroke.

6.4 Sickle cell disease and risk of arterial thrombosis

Sickle cell disease is associated with an increased risk of stroke in children (Adams *et al.*, 1998). Level I evidence has been established for the use of TCD in the diagnostic screening of patients with sickle cell anemia. A MCAv threshold of 170 cm/sec was identified as indicative for the need of blood transfusion, such that a 30% reduction in circulating hemoglobin-s was achieved (Adams *et al.*, 1997). A randomized trial subsequently demonstrated that application of the above Doppler criteria yielded a 92% absolute reduction in the risk of stroke in children (Adams *et al.*, 1998). Additionally, reference CBV values were recently outlined for the purpose of screening for intracranial vessel narrowing in children with sickle cell disease (Krejza *et al.*, 2000).

6.5 Brain death

Electroencephalography or angiography can be utilized for clinical diagnosis of brain death. Angiography is typically preferred because EEG gives little information regarding brainstem function and signals can be difficult to attain within the intensive care unit. However, angiography requires injectable contrast media, and cannot be completed bedside at all. Typically, increased intracranial pressure concomitant with brain death reduces diastolic blood flow velocity in the intracerebral vessels. Further increases in intracranial pressure produce reversed flow during diastole in the circle of Willis, and finally, spiked and reverberating flow is considered indicative of brain death (de Freitas & André, 2006; Ropper *et al.*, 1987; Tsivgoulis *et al.*, 2009).

6.6 Shunt and emboli detection

In the presence of right-to-left cardiac shunt microbubbles injected into the venous circulation – that are largely filtered out in the lungs – will appear in the cerebral circulation within 5-15 seconds. There are reports of up to 100% sensitivity in right-to-left shunt detection (Droste *et al.*, 2002); however, it seems unlikely that the TCD technique can

differentiate between various forms of shunt. For example, that microbubbles appear in the systemic circulation could be indicative of a patent foramen ovale, pulmonary arteriovenous malformation, or an atrial septal defect. But given that up to 60% of the normal population may present with right-to-left shunt of either intracardiac or pulmonary arteriovenous malformations (Woods *et al.*, 2010), an inexpensive means of screening such as TCD, as part of a diagnostic battery, may be very useful.

Both gaseous and solid microemboli can be detected using TCD through recognition of irregularities within the Doppler signal (Padayachee *et al.*, 1987; Deverall *et al.*, 1988; Ringelstein *et al.*, 1998). Although these microemboli are often clinically silent, their detection may be of prognostic value in assessing risk of stroke, and of use during cardiac or vascular surgeries where gaseous emboli may originate from the oxygenator. The detection of emboli using TCD is complicated and relies on 10 technical parameters and Ringelstein *et al*. provide a detailed description of the technique (Ringelstein *et al.*, 1998). There is some difficulty in distinguishing between gaseous and solid emboli. This is of clinical importance as each has distinct clinical relevance, particularly in cases where both types of emboli may be present (e.g., mechanical heart valve patients, patients with carotid stenosis (reviewed in: (Rodriguez *et al.*, 2009; Markus & Punter, 2005).

7. Utility of assessment of neck artery blood flow

Measurement of CBF by quantification of inflowing blood through the neck is not a new technique, but has not seen the prolific utilization of TCD or MRI, for example. Nonetheless, the technique has recently seen a resurgent popularity because it facilitates estimation of both flow proper (as opposed to blood velocity), and regional distribution of CBF during a variety of conditions (exercise, standing, environmental stress, etc.) not possible with MRI. The technique is nonetheless especially prone to measurement error, both for technical reasons and because of the apparent ease with which an untrained individual can pick up a vascular ultrasound probe, image a carotid artery, and believe the resulting measurement is accurate.

The aim of this section is to outline the virtues and caveats of the measurement of CBF via quantification of neck artery blood flow using high-resolution vascular ultrasound. First, we will discuss the vascular anatomy providing blood to the head. Then, we will address principals of linear vascular ultrasound, methods of analysis, sources of measurement error and our perspective on the appropriate use of the technique. Finally, the utility of the technique will be discussed in conjunction with an overview of the current literature.

7.1 The arteries of the neck

Early Greek physicians termed the principal arteries of the neck Karatides, after the adjective for stupefying, because their compression yielded unconsciousness. Such were these vessels' importance recognized early, even before the physiological function of blood was understood. Indeed, the carotid arteries are the principle conduit for blood transport to the brain, carrying approximately 70% of global CBF.

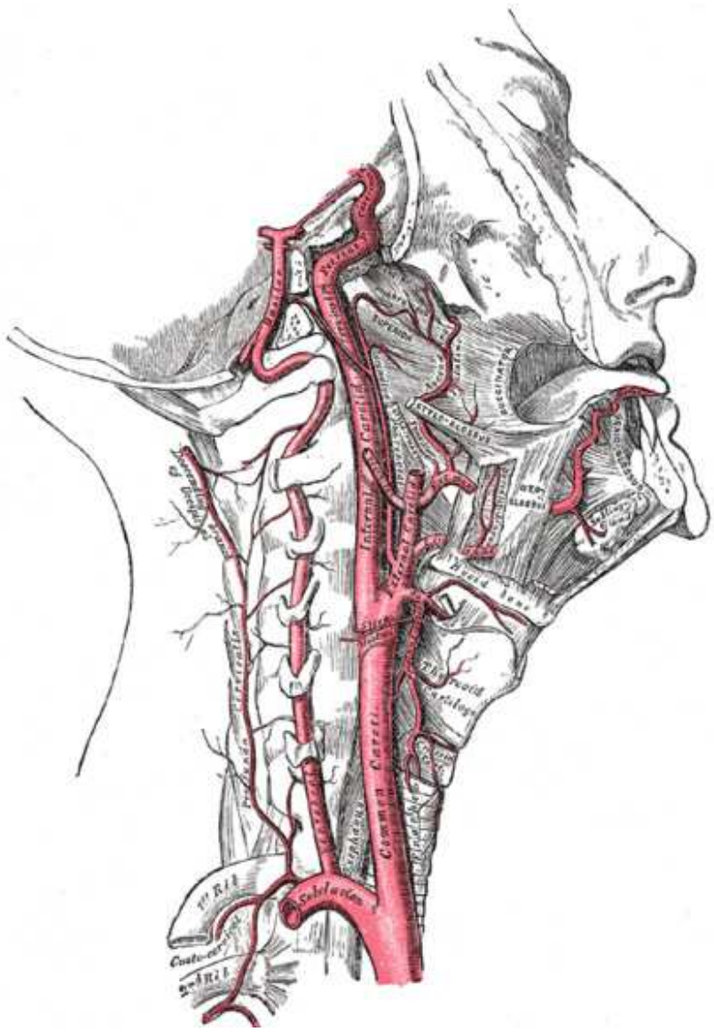

Fig. 7. Diagram of the right carotid arteries and vertebral artery.

The carotid system originates with the common carotid arteries (CCA), that branch from the aortic arch and brachiocephalic trunk on the left and right sides, respectively. The CCA bifurcates into the external (ECA) and internal (ICA) carotid arteries. The position and morphology of the carotid bifurcation exhibits some variation, lying somewhere between the level of the thyroid cartilage and hyoid bone in the majority of individuals. The ECA is most often positioned either anteromedial or medial to the ICA (Al-Rafiah *et al.*, 2011), giving off the superior thyroid artery and ascending pharangeal artery within the first two centimeters distal from the bifurcation. There is, however, variation in the loci of these arteries origins, occasionally branching from the CCA or ICA, and more often from the bifurcation itself. The ICA normally does not give off any branches until after entering the base of the skull through the foramen lacerum. The ophthalmic artery and a number of smaller arteries branch prior to the circle of Willis, where the ICA terminates to form the middle, anterior, and posterior communicating arteries. Because in the majority of individuals there are no branches off of the ICA prior to entering the skull, ICA blood flow is an accurate metric of CBF.

The vertebral arteries (VA) arise as the most proximal branches off the subclavian arteries, then course through the foremen of the transverse processes of C6-C2, into the spinal canal and skull to join bilaterally forming the basilar artery. The vessel can be imaged proximal to entering C6, and between each of the vertebra until entering the skull. There are numerous anastomoses with the VA both extra- and intracranially. The VA communicates with branches of the deep cervical artery, and inferior thyroid artery extracranially, and upon entering the skull gives off branches to the cerebellum before joining to form the basilar artery (BA). A number of arteries project from the BA to supply the cerebellum and pons before the BA bifurcates to form the poster circle of Willis as the posterior communicating arteries. The figure 8 below provide typical ultrasound example of the different waveforms commonly observed in the ICA, ECA and VA.

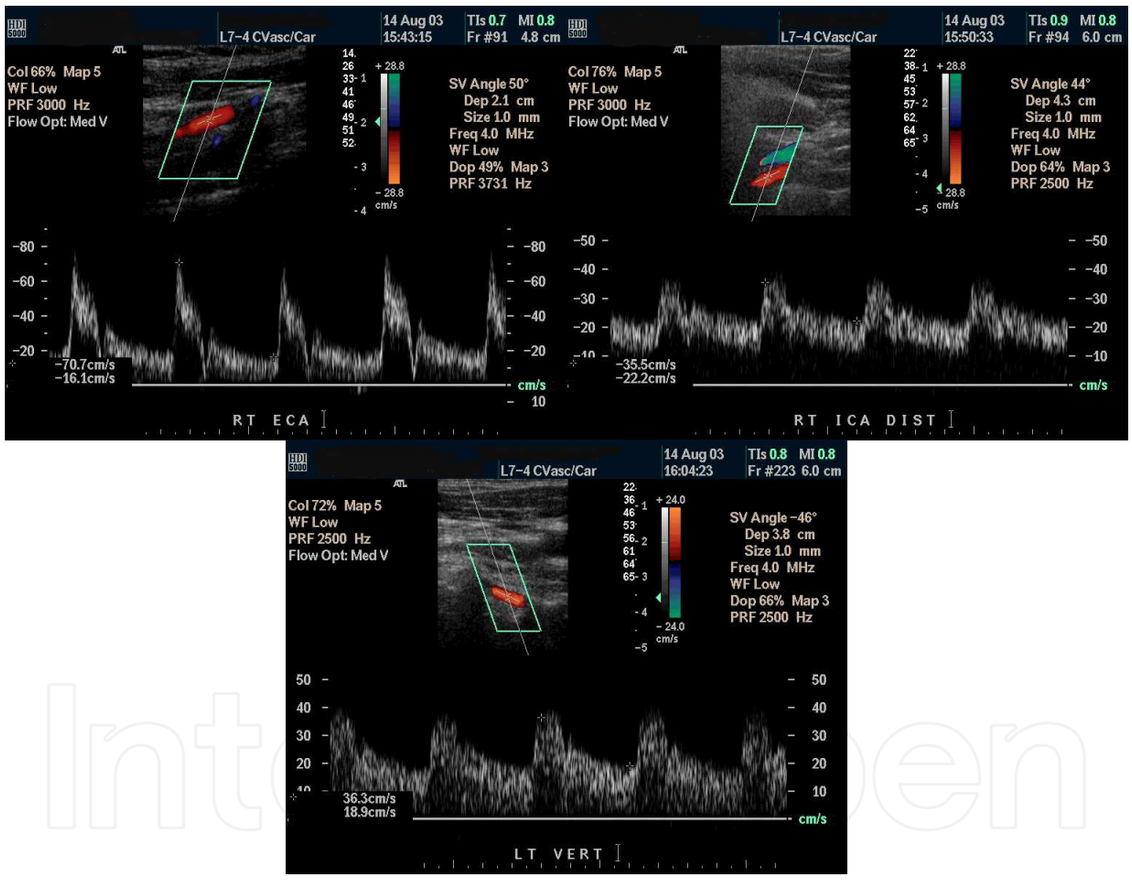

Fig. 8. From left to right, ultrasound examples of the ECA (left), ICA (middle) and VA (right). Note: 1) The ECA waveform should have a sharp upstroke and a low end-diastolic velocity, as it supplies a high resistance vascular bed. ECA may have a flow reversal component (flow below the baseline) in late systole or early diastole; 2) ICA waveform should have a more gradual upstroke (slower acceleration) in systole, and an elevated end-diastolic velocity. This is because it supplies a low resistance vascular bed (i.e., the brain). Thus flow should be above the baseline for the entire cardiac cycle; and 3) The VA waveform should have a gradual upstroke and relatively high end-diastolic velocity as it also supplies a low resistance vascular bed.

7.2 Technical aspects of vascular ultrasound

Neck artery ultrasound accurately quantifies global and regional CBF non-invasively and with high spatial and temporal resolution; indeed, it is the only known method of CBF measurement possessing these attributes. The principal limitation is consequently that of the operator, not the technique *per se.* But in fact the technique is so easily confounded by user error that this limitation obviates flippant dismissal. For example, a one degree error in the angle of insonation; a 0.1mm error in diameter measurement; and, one cm/s error in mean blood velocity each yield a 3, 4, and 4% error in the measurement of flow. It is obvious that very minor operator errors during insonation and during subsequent analysis quickly compound and can easily produce significant inaccuracies (Schoning *et al.*, 1994). For every 1-degree error in the insonation angle an approximate 3% error in velocity, and therefore in flow, results. But, whereas the velocity and flow error are linearly related, inaccuracies in the measurement of diameter have an exponentially larger effect (because the diameter is squared to calculate luminal area). The appropriate measurement of diameter is a topic of extensive debate within other fields reliant on ultrasonic measure of blood flow (Black *et al.*, 2008; Green *et al.*, 2011). It is unfortunate, then, that the accurate measurement of luminal diameter presents a number of problems that have largely been unaddressed since the invention of the technique. The majority of investigators utilize calipers typically part of the ultrasound software to manually measure from one luminal surface to the other. Some authors have accounted for the pulsatile nature of most arteries by measuring both systolic and diastolic diameters, and calculate a mean diameter based on a third to two-thirds systolic-diastolic ratio (Sato *et al.*, 2011; Sato & Sadamoto, 2010). Other authors have discordantly reported the ICA, ECA, and VA to be without pulsatile changes throughout the cardiac cycle (Scheel *et al.*, 2000a; Scheel *et al.*, 2000b; Schoning & Hartig, 1996; Schoning *et al.*, 2005a; Schoning *et al.*, 1994). Proprietary and commercially available software that automatically tracks the vessel internal walls on the B-mode image with high temporal resolution facilitates calculation of other metrics such as pulsatility and shear stress, and moreover dramatically increases the precision of the diameter measurement. Manual measurement of vessel lumen is also likely to prevent observation of any change in diameter, as arterial response to changes in shear or blood gases involves a temporal latency with stimulus related and inter –individual variability impossible to observe when only a few measures are taken.

8. Integrative assessment and future directions

Cerebrovascular function is clearly regulated by an array of functionally integrated processes. Measurement of only one process will provide an inadequate representation of this complex physiology. We therefore suggest that in both the research and clinical setting, assessment of cerebrovascular function with TCD should ideally include measures of four principle factors: (1) baseline CBV; (2) cerebrovascular reactivity; (3) cerebral autoregulation; and (4) neurovascular coupling. Furthermore, there is evidence that CBF and CA varies with time of day, exercise, body position, caffeine, food intake, and menstrual cycle; as such, these variables should be carefully standardized for each of the following metrics both between and within subjects or patients.

8.1 Baseline cerebral blood flow and velocities in arteries of interest

Because normative data for blood flow velocities is well known within the literature for the MCA (Aaslid *et al.*, 1984; Ringelstein *et al.*, 1990) and related neck arteries (Scheel *et al.*, 2000b; Schoning *et al.*, 1994); thus, baseline blood flow and CBFv should always be collected for all arteries of interest. Indeed, diagnosis of atypical flow patterns within the cerebral circulation is indicative of a number of conditions such as intracerebral stenosis or occlusion (Aaslid, 1986b; Aaslid, 2006). Because in a normal population cerebrovascular function is largely determined by its ability to adjust to changes in perfusion pressure, it is largely the change from baseline following a stimulus that is of greatest importance in assessing autoregulation.

8.2 Cerebrovascular reactivity

Cerebrovascular reactivity is an accepted independent predictor of ischemic stroke (Markus & Cullinane, 2001). That it has been linked with a spectrum of vascular pathologies justifies its inclusion when assessing cerebrovascular function. Arterial CO_2 can be increased through inhalation of a hypercapnic gas or simple re-breathing paradigm. Ainslie & Duffin (2009) have recently detailed the assessment and related interpretation of cerebrovascular reactivity. Furthermore, $PetCO_2$ should always be measured because of its direct effects on cerebrovascular calibre. Moreover, spontaneous measures of *d*CA are affected differentially by hypercapnia and hypocapnia (Panerai *et al.*, 1999b).

8.3 Cerebral autoregulation

Quantification of cerebral autoregulation (CA) is clearly an important factor in any study assessing cerebrovascular function. Despite caveats inherent to each methods of CA quantification most studies to date have applied only one measure of CA, and generally in the hypotensive range. Moreover, recent studies have largely focused on spontaneous CA analysis using TFA. However, we recommend that it is critical to 'force' the BP challenge in order to reliably engage CA. Driving BP oscillations using either squat-stand, or oscillating lower body negative pressure at the frequency of interest will enhance the reliability and validity of TFA measures (Claassen *et al.*, 2009; Hamner *et al.*, 2004). Like the Oxford method, this approach also permits the assessment and separation of the cerebral responses to both hypotension and hypertension. Given the apparent difference in efficacy of CA to managing falling or rising perfusion pressures, and the distinct consequences to dysregulation (i.e., ischemia versus hemorrhage, respectively), this is an important consideration.

8.4 Neurovascular coupling

Neurovascular coupling (NVC) is likely involved in maintenance of adequate nutrient and oxygen supply to specific regions of the brain. It is a relatively simple addition to any experimental design, and should be measured if time permits. The regional task specificity within the brain allows coupling to be easily assessed; simple sensory stimuli (e.g., turning on a light) provides adequate stimulus to assess neurovascular coupling in the cortex by measurement of CBV in the PCA (Aaslid, 1987). Coupling between neural activity is decreased in a number of pathologies, including hypertension, Alzheimer's disease, ischemic stroke (reviewed by Girouard & Iadecola, 2006), and in long-term smokers (Woods *et al.*, 2010).

9. TCD and neck blood flow utility

It is clear that there is tremendous utility in the assessment of cerebrovascular function with TCD. Surprisingly, integrative assessment of cerebrovascular function is currently lacking and no studies to date have combined the assessment of these four fundamental measurements. Given that regulation of cerebrovascular function involves the complex integration of each of the above factors, only experimental designs that incorporate holistic assessment of multiple mechanisms can hope to clarify the complex physiology responsible for maintaining brain O_2 and nutrient delivery in such narrow margins.

In the clinical setting, depending on the key measurement question, the implementation of a simplified protocol that encompasses each of these metrics is prudent. Measurement of MCAv, PCAv, ECG, beat-to-beat BP, and end-tidal gases should be recorded throughout. The following protocol would likely be adequate: 5 minutes supine baseline; 2 minutes eyes closed; 2 minutes of reading followed by 5-10 cycles of 20 seconds eyes closed followed by 40 seconds reading to assess NVC; 2 minutes of either rebreathing or breathing of a 5% CO2 gas mixture to assess cerebrovascular reactivity; and finally one BP stimulus - either using the Oxford technique, thigh cuffs, Valsalva maneuver, or squat-stand cycles. Such a protocol, with one or two skilled experimenters, can be completed within 45-60 minutes on both healthy subjects and a variety of patient groups (Figure 9).

The prototype for the assessment of both blood velocity and vessel diameter was introduced in 1974 (Barber *et al.*, 1974). Several years later pulsed-Doppler ultrasound was utilized for the quantification of blood velocity in the internal carotid and vertebral arteries during changes in inspired CO_2 (Hauge *et al.*, 1980). This early technology lacked B-mode functionality to allow visualization of the vessel, and measurement of diameter. Consequently, the diameter of the vessel had to be assumed constant for the velocity to be indicative of flow, a problem overcome several years later following diagnostic utilization of combined B-mode and Doppler (Duplex) scanning for identification of artherosclerotic pathology (Blackshear *et al.*, 1979; Strandness, 1985). The "logical progression" came soon after when Leopold et al (1987) applied Duplex scanning to the internal carotid artery to quantify CBF and CO_2 reactivity. The method's principal use has since been for the evaluation of neck artery pathology, however a handful of studies have utilized the technique for the quantification of CBF decline through aging (Schoning & Hartig, 1996; Schoning *et al.*, 1994) and to assess cerebrovascular reactivity to CO_2 and O_2 (Fortune *et al.*, 1992; Hauge *et al.*, 1980; Leopold *et al.*, 1987; Schoning *et al.*, 1994). The results of these studies are broadly consistent with studies assessing cerebrovascular reactivity and global brain blood flow using indicator dilution techniques (Ainslie & Duffin, 2009; Battisti *et al.*, 2010; Fan *et al.*, 2008) (Ackerman *et al.*, 1973; Grubb *et al.*, 1974; Harper & Glass, 1965), and TCD.

Use of ICA blood flow has been extended to the bedside diagnostic assessment of myriad cerebrovascular pathologies. There is a small body of literature describing insonation of the ICA for the assessment of periventricular leukomlacia (Kehrer & Schoning, 2009), cerebral vasculitis (Kamm *et al.*, 2008; Kuker *et al.*, 2008), evaluation of cerebral circulatory arrest (Schoning *et al.*, 2005b), and for establishing normative values for CBF during natal development (Kehrer *et al.*, 2005; Kehrer & Schoning, 2009). Ultrasonic study of the vertebral arteries has also received attention with respect to risk identification involved with

chiropractic cervical spine manipulation (Bowler *et al.*, 2011; Mitchell, 2005), though many of the conclusions herein remain speculative.

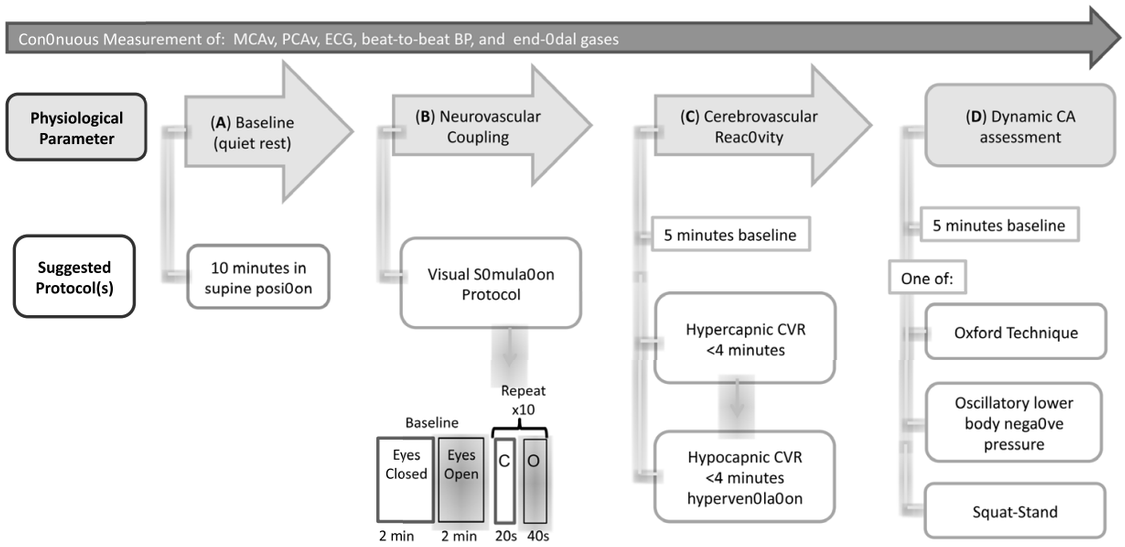

Fig. 9. (A) A complete resting assessment of intracranial blood flow using TCD should include blood velocities of middle cerebral artery (MCA), posterior cerebral artery (PCA), anterior cerebral artery (ACA) and basilar artery. The probe(s) can then be fixed on the arteries of interest for the remainder of the protocol. Electrocardiogram, end-tidal gases, and beat-to-beat blood pressure should be measured concomitantly with cerebral blood velocity metrics throughout the experiment. (B) The neurovascular coupling protocol should consist of 2 minutes each of resting with eyes open and closed, followed by 5-10 cycles of 20 seconds eyes closed and 40 seconds of reading with concurrent measurement of MCA and PCA velocities. (C) Assessment of cerebrovascular reactivity in both hypercapnic and hypocapnic ranges can be carried out in <4 minutes of rebreathing or inhalation of 5% CO_2, or, hyperventilation, respectively. (D) Dynamic cerebral autoregulation can be assessed using any of: supra-systolic thigh-cuff release (Section 5.1), the Valsalva maneuver (Section 5.3), the Oxford technique, or oscillatory blood pressure perturbations. The Oxford technique (Section 5.5) or transfer function analysis using either squat-stand cycles or oscillating lower body negative pressure at 0.05 and 0.1 Hz are recommended for reasons detailed in Section 5.6 and Figure 5.

More recently neck artery blood flow quantification has seen a resurgent application in physiology research. Sato et al conducted two studies (Bowler *et al.*, 2011; Mitchell, 2005; Sato *et al.*, 2011; Sato & Sadamoto, 2010) utilizing the technique to quantify changes in regional head perfusion during varying degrees of semi-recumbent cycling exercise. They measured blood flow in the external, internal, and common carotid arteries, as well as in the vertebral artery to show that the well-documented increase-plateau-decrease with progressive exercise to intensities above the ventilator threshold was only evident in the anterior circulation. Their data indicate, and support previous suggestions, that the poster and anterior cerebral circulations possess disparate blood flow regulation and CO_2

sensitivities. In this respect the possibility that the arteries of the neck were directly involved in the regulation of CBF was raised by their data (Hellström *et al.*, 1996).

From an integrative systems approach, numerous factors independently, synergistically, and sometimes antagonistically participate in the regulation of CBF. In addition to the traditional mechanisms describing CBF regulation (e.g. autoregulation, partial pressure of arterial carbon dioxide), a variety of other factors, such as cardiac output, the arterial baroreflex and chemoreflex control, are very likely involved in this complex regulatory physiology. Research exploring these complex interactions, especially in relation to neurovascular coupling, is currently lacking. Future studies with particular focus on these integrative physiological mechanisms are clearly warranted in both health and disease states.

10. Conclusions

Many methods are available for the assessment of CBF, but the high temporal resolution, non-invasiveness, and relative low-cost of TCD make it functional in both clinical and research settings. The ability to assess cerebral reactivity, CA, and neurovascular coupling, makes TCD extremely useful for the assessment of integrative cerebrovascular function. Four principle components of cerebrovascular regulation can, and should, be assessed using TCD, as collectively these provide insight into a complex physiology. Measurement of (1) velocities within the major cerebral vessels; (2) measurement of ICA, ECA and VA blood flow, (3) assessments of autoregulation, (4) cerebrovascular reactivity and (5) neurovascular coupling together facilitate holistic appraisal of cerebrovascular function.

11. Appendix

Methodology				Blood Flow Parameters							
Study	**Intervention**	**Imaging Technique**	**Analysis Method**	**Vessel**	**PSV (cm/s)**	**EDV (cm/s)**	**Vmean (cm/s)**	**Diameter (mm)**	**Blood Flow (ml/min)**	**Other**	
	Resting Studies										
Yazici *et al.*, 2005	Rest	Duplex ultrasound	CCA measurements taken 2 cm proximal to the bifurcation; ICA and ECA measurements taken 1-2 cm distal to the bifurcation; VA measurements taken bilaterally between the 4th and 5th cervical vertebral transverse processes in the sagittal plane. B-mode images. Age is presented in parentheses. (*n*=96)	CCA (21-50)	98 ± 20	26 ± 6		6.2 ± 0.6	427 ± 106		
				CCA (51-80)	74 ± 15	20 ± 5		6.8 ± 0.8	408 ± 95		
				ECA (21-50)	71 ± 15	16 ± 5		4.1 ± 0.5	128 ± 45		
				ECA (51-80)	73 ± 19	14 ± 5		4.1 ± 0.7	139 ± 57		
				ICA (21-50)	76 ± 14	30 ± 7		4.5 ± 0.5	238 ± 57		
				ICA (51-80	65 ± 14	25 ± 6		4.6 ± 0.7	225 ± 60		
				VA (21-50)	53 ± 10	18 ± 5		3.5 ± 0.4	86 ± 34		
				VA (51-80)	48 ± 12	15 ± 17		3.6 ± 0.5	77 ± 41		
										CBF volume (ml/min)	
										Combined	**Male**	**Female**
Scheel *et al.*, 2000	Rest	Duplex ultrasound	Flow volume measurements were in the C4-C5 inter-transverse segment of the VA, 1.5-2 cm below the carotid bulb in the ECA and ICA. Luminal diameter determined on the enlarged B-mode. Angle of insonation = ~60°. 3-5 cardiac cycles. Age is presented in parentheses. (*n*=78).	VA (20-85)					158 ± 48	657 ±120	670 ± 117	644 ± 123
				VA (20-39)					173 ± 41	727 ± 102	725 ± 87	730 ± 87
				VA (40-59)					147 ± 36	656 ± 121	663 ± 126	648 ± 120
				VA (60-85)					155 ± 58	603 ± 106	648 ± 120	572 ± 99
				ICA (20-85)					499 ± 108			
				ICA (20-39)					554 ± 99			
				ICA (40-59)					508 ± 114			
				ICA (60-85)					448 ± 85			
				ECA (20-85)					328 ± 111			
				ECA (20-39)					290 ± 63			
				ECA (40-59)					350 ± 146			
				ECA (60-85)					340 ± 103			
				CCA (20-85)					816 ± 198			
				CCA (20-39)					853 ± 197			
				CCA (40-59)					868 ± 223			
				CCA (60-85)					745 ± 160			

Scheel *et al.*, 2000	Rest	Colour duplex sonography	Flow volume measurements were most frequently taken in the C4-C5 intertransverse segment of the VA, 1.5 -2 cm below the carotid bulb in the CCA, and 1-2 cm above the carotid bulb in ECA and ICA. D = B-mode; measure diameter of CCA in end-diastolic phase. Angle of insonation = 60°. Age is presented in parentheses. (*n*=78).	CCA (20-39)	101 ± 22	25 ± 5	25 ± 5	6.0 ± 0.7	426 ± 99	
				CCA (40-59)	89 ± 17	26 ± 5	25 ± 5	6.1 ± 0.8	434 ± 111	
				CCA (60-85)	81 ± 21	20 ± 7	21 ± 6	6.2 ± 0.9	373 ± 80	
				ECA (20-39)	86 ± 14	16 ± 4	19 ± 3	4.0 ± 0.4	145 ± 32	
				ECA (40-59)	85 ± 18	19 ± 3	22 ± 5	4.1 ± 0.7	175 ± 73	
				ECA (60-85)	81 ± 30	15 ± 6	20 ± 7	4.3 ± 0.7	170 ± 73	
				ICA (20-39)	72 ± 18	26 ± 5	26 ± 5	4.8 ± 0.5	277 ± 49	
				ICA (40-59)	65 ± 10	26 ± 5	25 ± 5	4.7 ± 0.6	254 ± 57	
				ICA (60-85)	58 ± 11	20 ± 5	21 ± 6	4.9 ± 0.8	224 ± 43	
				VA (20-39)	52 ± 6	17 ± 3	17 ± 3	3.3 ± 0.3	87 ± 20	
				VA (40-59)	47 ± 8	15 ± 3	14 ± 2	3.2 ± 0.4	74 ± 18	
				VA (60-85)	45 ± 11	12 ± 3	12 ± 4	3.6 ± 0.4	78 ± 29	
Schoning & Hartig, 1996	Rest	Duplex ultrasound	CCA measurements taken 1.5-2 cm proximal to bifurcation . ICA and ECA measurements taken 1.5-2 cm distal to bifurcation. VA measurements taken between C4-C5 vertebral transverse process. B-mode imaging. Age is presented in parentheses. (*n*=94).	CCA (3-9.9)					775 ± 117	
				CCA (10-18)					750 ± 119	
				ECA (3-9.9)					113 ± 43	
				ECA (10-18)					189 ± 64	
				ICA (3-9.9)					585 ± 90	
				ICA (10-18)					543 ± 90	
				VA (3-9.9)					236 ± 51	
				VA (10-18)					184 ± 36	
				CBFV (3-9.9)					821 ± 116	
				CBFV (10-18)					727 ± 106	
									Blood Flow (ml/min)	
									Observer A	**Observer B**
Schoning & Scheel, 1996	Rest	Doppler flowmetry and colour duplex sonography	ECA and ICA measurements taken 1.5-2 cm above the bifurcation. B-mode to take luminal diameter. (*n*=32).	LICA Day 1					276 ± 68	266 ± 63
				RICA Day 1					268 ± 54	260 ± 57
				LICA Day 2					269 ± 65	257 ± 52
				RICA Day 2					254 ± 60	249 ± 44
				LVA Day 1					99 ± 44	97 ± 44
				RVA Day 1					74 ± 38	79 ± 41
				LVA Day 2					94 ± 41	92 ± 38
				RVA Day 2					75 ± 38	74 ± 36
				CBFV Exam 1					723 ± 153	699 ± 155
				CBFV Exam 2					709 ± 146	694 ± 146
				CBFV Exam 3					693 ± 136	672 ± 110
Schoning *et al.*, 1994	Rest	Duplex ultrasonography	Measurements taken 1.5 cm below carotid bulb in the CCA and 1.0 to 1.5 cm away from the bifurcation in ICA and ECA. VA was measured at the C4-C5 intertransverse area. D = B-mode ICA, ECA and VA; M-mode for CCA. (*n*=48).	CCA	96 ± 25	26 ± 6	25.4 ± 5.4	6.3 ± 0.9	470 ± 120	
				ICA	66 ± 16	26 ± 6	24.9 ± 5.2	4.8 ± 0.7	265 ± 62	
				ECA	83 ± 17	17 ± 5	19.6 ± 4.1	4.1 ± 0.6	160 ± 66	
				VA	48 ± 10	16 ± 4	15.6 ± 3.6	3.4 ± 0.6	85 ± 33	
	Exercise Studies									
Sato *et al.*, 2011	Rest	Duplex ultrasound	Measurements for the ICA were taken 1.0-1.5 cm distal to bifurcation on the left ICA, chin slightly elevated; VA measured between the transverse process of the C3 and subclavian artery. Left ECA and right CCA measured 1.0-1.5 cm above the carotid. Mean diameter = [(systolic diameter x 1/3)] + [(diastolic diameter x 2/3)]. (*n*=10).	CCA			28.5 ± 1.0	5.2 ± 0.1	363 ± 18	
				ICA			28.4 ± 1.3	4.2 ± 0.1	239 ± 14	
				ECA			19.6 ± 1.6	3.8 ± 0.1	129 ± 12	
				VA			20.1 ± 1.0	3.1 ± 0.2	90 ± 12	
	40% VO_2 Peak			CCA			31.3 ± 0.7	5.3 ± 0.1	420 ± 14	
				ICA			33.7 ± 1.3	4.2 ± 0.1	280 ± 14	
				ECA			24.2 ± 1.9	3.9 ± 0.1	163 ± 10	
				VA			25.2 ± 2.5	3.1 ± 0.2	117 ± 13	
	60% VO_2 Peak			CCA			34.2 ± 1.0	5.4 ± 0.1	463 ± 20	
				ICA			34.4 ± 1.6	4.2 ± 0.1	291 ± 16	
				ECA			25.6 ± 2.2	4.0 ± 0.1	183 ± 12	
				VA			27.8 ± 1.9	3.1 ± 0.2	129 ± 12	
	80% VO_2 Peak			CCA			35.9 ± 1.2	5.4 ± 0.1	500 ± 31	
				ICA			30.4 ± 1.0	4.2 ±0.1	258 ± 13	
				ECA			31.8 ± 2.2	4.0 ± 0.1	238 ± 13	
				VA			30.3 ± 2.0	3.2 ± 0.2	144 ± 14	

Sato *et al.*, 2009	Voluntary elbow flexion/ extension (no load; 2 min)	Duplex ultrasound	Motor-driven lever arm rotated at constant velocity. Measured vessel diameter and blood flow velocity at 2-3 cm proximal to the carotid bifurcation using an insonation angle as low as possible <60° (*n*=11).	CCA			23,9 ± 2,6	378 ± 41
	Passive mechanoreflex activating elbow extension			CCA			24.2 ± 3.2	370 ± 43
Hellstrom *et al.*, 1996	Rest	Duplex ultrasonography	5- to 10-MHz-wide band linear-array transducer. Vessel diameter measured in B mode. M-mode for use in flow calculations. Increase exercise workload every 6 min. Ergometer cycle. (*n*=11).	CCA				591 ± 200
	20-22% VO_2 max			CCA				610 ± 200
	40-44%VO_2 max			CCA				698 ± 399
	60-67% VO_2 max			CCA				784 ± 300
	80-90% VO_2 max			CCA				839 ± 300
	Rest			CCA				752 ± 200
	Rest			ICA				332 ± 50
	20-22% VO_2 max			ICA				366 ± 60
	40-44%VO_2 max			ICA				367 ± 60
	60-67% VO_2 max			ICA				387 ± 70
	80-90% VO_2 max			ICA				360 ± 70
	Rest			ICA				340 ± 70
	Postitional Studies							
Bowler *et al.*, 2011	Neutral	Duplex ultrasound	Doppler angle = 56°. Measurements ICA 1-2 cm above the carotid bulb (C2/3); VA measured at C2/3. Vmean = [(PSV - EDV)/3] + EDV. (*n*=14).	LICA	92.4 ± 22.4	33.6 ± 6.8	53.2 ± 11.4	
				RICA	98.8 ± 21.7	38.2 ± 7.0	58.4 ± 10.5	
				LVA	55.0 ± 9.5	18.5 ± 3.0	30.7 ± 4.6	
				RVA	54.1 ± 18.7	18.0 ± 5.7	30.0 ± 9.8	
	SMP (LR,RSF)			LICA	95.2 ±19.2	39.7 ± 9.2	58.2 ± 11.5	
				RICA	96.4 ± 19.7	36.3 ± 7.1	56.3 ± 10.1	
				LVA	50.6 ± 11.7	18.3 ± 3.9	29.1 ± 6.3	
				RVA	45.9 ± 8.6	17.5 ± 4.4	26.9 ± 5.3	
	Neutral			LICA	95.7 ± 20.1	36.0 ± 7.7	55.9 ± 10.5	
				RICA	96.7 ± 17.1	35.9 ± 6.3	56.1 ± 7.3	
				LVA	57.1 ± 13.7	20.2 ± 4.4	32.5 ± 6.7	
				RVA	53.2 ± 16.3	19.3 ± 7.0	30.6 ±9.9	
	SMP (RR, LSF)			LICA	91.2 ± 22.5	32.7 ± 7.6	52. 2 ± 11.2	
				RICA	100.6 ± 23.4	37.3 ± 11.3	58.4 ± 13.4	
				LVA	54.5 ± 14.0	19.0 ± 4.2	30.8 ± 7.0	
				RVA	50.3 ± 15.8	19.5 ± 7.5	29.8 ± 10.1	
	Pharmaceutical Studies							
Bokker *et al.*, 2011	Pre-acetazolamide	Arterial spin labelling; 3T MRI scanner.	For positioning at low-resolution T1-weighted spin-echo sequence was obtained in the sagittal plane. Perfusion images consisted of 17 7 mm slices aligned parallel to the orbitomeatal angle, acquired in ascending fashion with an in-plance resolution 3x3 mm 9 true acquisition resolution. (*n*=16).	ICA				51.8 ± 8.1
	Post-acetazolamide			ICA				78.6 ± 12.4
	Pathological Studies							
Albayrak *et al.*, 2006	Healthy	Duplex ultrasound	Measurements for ICA 1.5 cm distal to the carotid bifurcation. VA examined between the transverse processes of the vertebrae C4 and C5. TAV = integral of the mean flow velocities of all moving particles passing the sample volume over 3-5 complete cardiac cycles. (*n*=29).	LICA	51.8 ±14.9	18.1 ± 6.6		
				RICA	54.4 ± 14.4	18.1 ± 5.2		
				LVA	37.7 ± 12.1	11.3 ± 5.6		
				RVA	36.6 ± 11.3	10.3 ± 4.5		
	COPD			LICA	62.1 ± 18.9	18.9 ± 6.7		
				RICA	54.5 ± 18.3	16.9 ± 5.4		
				LVA	40.9 ± 12.5	11.7 ± 4.8		
				RVA	38.4 ± 13.9	9.9 ± 4.3		

Abbreviations: CBFV; cerebral blood flow volume. CCA; common carotid artery.
COPD; chronic obstrutive pulmonary disease. ECA; external carotid artery.
EDV; end-diastolic velocity. ICA; internal carotid artery. LICA; left internal carotid artery.
LVA; left vertebral artery. PSV; peak systolic velocity. RICA; right intrnal carotid artery.
RVA; right vertrbral artery. SMP; simulated manipulation position
[LR, RSF; left rotation, right side flexion or RR, LSF; right rotation, left side flexion].
TAV; time averaged maximum blood flow velocity, VA; vertebral artery.
Vmean; mean velocity

12. References

Aaslid R (1986a). The Doppler principle applied to measurement of blood flow velocity in cerebral arteries. In *Transcranial Doppler sonography* ed. Aaslid R, Springer-Verlag, New York.

Aaslid R (1986b). Transcranial Doppler Examination Techniques. In *Transcranial Doppler Sonography* ed. Aaslid R, pp. 39–59. Springer-Verlag, New York.

Aaslid R (1987). Visually evoked dynamic blood flow response of the human cerebral circulation. *Stroke* 18, 771–775.

Aaslid R (2006). Cerebral autoregulation and vasomotor reactivity. *Frontiers of neurology and neuroscience* 21, 216–228.

Aaslid R, Blaha M, Sviri G, Douville CM & Newell DW (2007). Asymmetric dynamic cerebral autoregulatory response to cyclic stimuli. *Stroke* 38, 1465–1469.

Aaslid R, Huber P & Nornes H (1984). Evaluation of cerebrovascular spasm with transcranial Doppler ultrasound. *J Neurosurg* 60, 37–41.

Aaslid R, Lash SR, Bardy GH, Gild WH & Newell DW (2003). Dynamic pressure--flow velocity relationships in the human cerebral circulation. *Stroke* 34, 1645–1649.

Aaslid R, Lindegaard KF, Sorteberg W & Nornes H (1989). Cerebral autoregulation dynamics in humans. *Stroke* 20, 45–52.

Aaslid R, Markwalder TM & Nornes H (1982). Noninvasive transcranial Doppler ultrasound recording of flow velocity in basal cerebral arteries. *J Neurosurg* 57, 769–774.

Ackerman RH, Zilkha E, Bull JW, Du Boulay GH, Marshall J, Russell RW & Symon L (1973). The relationship of the CO 2 reactivity of cerebral vessels to blood pressure and mean resting blood flow. *Neurology* 23, 21–26.

Adams RJ, McKie VC, Carl EM, Nichols FT, Perry R, Brock K, McKie K, Figueroa R, Litaker M, Weiner S & Brambilla D (1997). Long-term stroke risk in children with sickle cell disease screened with transcranial Doppler. *Ann Neurol* 42, 699–704.

Adams RJ, McKie VC, Hsu L, Files B, Vichinsky E, Pegelow C, Abboud M, Gallagher D, Kutlar A, Nichols FT, Bonds DR & Brambilla D (1998). Prevention of a first stroke by transfusions in children with sickle cell anemia and abnormal results on transcranial Doppler ultrasonography. *N Engl J Med* 339, 5–11.

Ainslie P & Duffin J (2009). Integration of cerebrovascular CO2 reactivity and chemoreflex control of breathing: mechanisms of regulation, measurement, and interpretation. *AJP: Regulatory, Integrative and Comparative Physiology* 296, R1473–R1495.

Ainslie P & Tzeng Y (2010). On the regulation of the blood supply to the brain: old age concepts and new age ideas. *Journal of Applied Physiology* 108, 1447–1449.

Ainslie PN & Ogoh S (2010). Regulation of cerebral blood flow in mammals during chronic hypoxia: a matter of balance. *Exp Physiol* 95, 251–262.

Al-Rafiah A, EL-Haggagy AA, Aal IH & Zaki AI (2011). Anatomical study of the carotid bifurcation and origin variations of the ascending pharyngeal and superior thyroid arteries. *Folia Morphol (Warsz)* 70, 47–55.

Alexandrov AV (2006). Ultrasound enhanced thrombolysis for stroke. *International journal of stroke : official journal of the International Stroke Society* 1, 26–29.

Alexandrov AV (2009). Ultrasound enhancement of fibrinolysis. *Stroke* 40, S107–10.

Alexandrov AV, Molina CA, Grotta JC, Garami Z, Ford SR, Alvarez-Sabin J, Montaner J, Saqqur M, Demchuk AM, Moyé LA, Hill MD, Wojner AW & Investigators

CLOTBUST (2004). Ultrasound-enhanced systemic thrombolysis for acute ischemic stroke. *N Engl J Med* 351, 2170–2178.

Barber FE, Baker DW, Nation AW, Strandness DEJ & Reid JM (1974). Ultrasonic duplex echo-Doppler scanner. *IEEE Trans Biomed Eng* 21, 109–113.

Battisti A, Fisher JA & Duffin J (2010). Measuring the hypoxic ventilatory response. *Advances in experimental medicine and biology* 669, 221–224.

Bishop CC, Powell S, Rutt D & Browse NL (1986). Transcranial Doppler measurement of middle cerebral artery blood flow velocity: a validation study. *Stroke* 17, 913–915.

Black MA, Cable NT, Thijssen DH & Green DJ (2008). Importance of measuring the time course of flow-mediated dilatation in humans. *Hypertension* 51, 203–210.

Blackshear WMJ, Phillips DJ, Thiele BL, Hirsch JH, Chikos PM, Marinelli MR, Ward KJ & Strandness DEJ (1979). Detection of carotid occlusive disease by ultrasonic imaging and pulsed Doppler spectrum analysis. *Surgery* 86, 698–706.

Boms N, Yonai Y, Molnar S, Rosengarten B, Bornstein NM, Csiba L & Olah L (2010). Effect of smoking cessation on visually evoked cerebral blood flow response in healthy volunteers. *J Vasc Res* 47, 214–220.

Bowler N, Shamley D & Davies R (2011). The effect of a simulated manipulation position on internal carotid and vertebral artery blood flow in healthy individuals. *Man Ther* 16, 87–93.

Brassard P, Seifert T, Wissenberg M, Jensen P, Hansen C & Secher N (2010). Phenylephrine decreases frontal lobe oxygenation at rest but not during moderately intense exercise. *Journal of Applied Physiology* 108, 1472–1478.

Bruneau N, Dourneau MC, Garreau B, Pourcelot L & Lelord G (1992). Blood flow response to auditory stimulations in normal, mentally retarded, and autistic children: a preliminary transcranial Doppler ultrasonographic study of the middle cerebral arteries. *Biol Psychiatry* 32, 691–699.

Burgess KR, Fan JL, Peebles K, Thomas K, Lucas S, Lucas R, Dawson A, Swart M, Shepherd K & Ainslie P (2010). Exacerbation of obstructive sleep apnea by oral indomethacin. *Chest* 137, 707–710.

Camerlingo M, Casto L, Censori B, Ferraro B, Gazzaniga GC & Mamoli A (1993). Transcranial Doppler in acute ischemic stroke of the middle cerebral artery territories. *Acta Neurol Scand* 88, 108–111.

Cassaglia P, Griffiths R & Walker A (2009). Cerebral sympathetic nerve activity has a major regulatory role in the cerebral circulation in REM sleep. *Journal of Applied Physiology* 106, 1050–1056.

Cassaglia PA, Griffiths RI & Walker AM (2008). Sympathetic withdrawal augments cerebral blood flow during acute hypercapnia in sleeping lambs. *Sleep* 31, 1729–1734.

Chapman RW, Santiago TV & Edelman NH (1979). Effects of graded reduction of brain blood flow on chemical control of breathing. *Journal of applied physiology: respiratory, environmental and exercise physiology* 47, 1289–1294.

Claassen JA, Levine BD & Zhang R (2009). Dynamic cerebral autoregulation during repeated squat-stand maneuvers. *J Appl Physiol* 106, 153–160.

Czosnyka M, Brady K, Reinhard M, Smielewski P & Steiner LA (2009). Monitoring of cerebrovascular autoregulation: facts, myths, and missing links. *Neurocritical care* 10, 373–386.

de Freitas GR & André C (2006). Sensitivity of transcranial Doppler for confirming brain death: a prospective study of 270 cases. *Acta Neurol Scand* 113, 426–432.

Deegan BM, Devine ER, Geraghty MC, Jones E, Olaighin G & Serrador JM (2010). The relationship between cardiac output and dynamic cerebral autoregulation in humans. *J Appl Physiol* 109, 1424–1431.

Deppe M, Ringelstein EB & Knecht S (2004). The investigation of functional brain lateralization by transcranial Doppler sonography. *Neuroimage* 21, 1124–1146.

Deverall PB, Padayachee TS, Parsons S, Theobold R & Battistessa SA (1988). Ultrasound detection of micro-emboli in the middle cerebral artery during cardiopulmonary bypass surgery. *Eur J Cardiothorac Surg* 2, 256–260.

DeWitt LD & Wechsler LR (1988). Transcranial Doppler. *Stroke* 19, 915–921.

Dorst J, Haag A, H. OW, Hamer HM & Rosenow F (2008). Functional transcranial Doppler sonography and a spatial orientation paradigm identify the non-dominant hemisphere. *Brain and cognition* 68, 53–58.

Droste DW, Lakemeier S, Wichter T, Stypmann J, Dittrich R, Ritter M, Moeller M, Freund M & Ringelstein EB (2002). Optimizing the technique of contrast transcranial Doppler ultrasound in the detection of right-to-left shunts. *Stroke* 33, 2211–2216.

Duschek S, Hadjamu M & Schandry R (2007). Enhancement of cerebral blood flow and cognitive performance following pharmacological blodd pressure elevation in chronic hypotension. *Psychophysiology* 44, 145–153.

Duschek S, Heiss H, Werner N & Reyes del Paso GA (2009). Modulations of autonomic cardiovascular control following acute alpha-adrenergic treatment in chronic hypotension. *Hypertens Res* 32, 938–943.

Duschek S & Schandry R (2007). Reduced brain perfusion and cognitive performance due to constitutional hypotension. *Clin Auton Res* 17, 69–76.

Duschek S, Werner N, Kapan N & Reyes del Paso GA (2008). Patterns of cerebral blood flow and systemic hemodynamics during arithmetic processing. *Journal of Psychophysiology* 22, 81–90.

Eckberg DL (1980). Nonlinearities of the human carotid baroreceptor-cardiac reflex. *Circ Res* 47, 208–216.

Edvinsson L & Krause DN (2002). Lippincott, Williams & Wilkins, Philadelphia.

Eggers J, Koch B, Meyer K, König I & Seidel G (2003). Effect of ultrasound on thrombolysis of middle cerebral artery occlusion. *Ann Neurol* 53, 797–800.

Eggers J, Ossadnik S & Seidel G (2009). Enhanced clot dissolution in vitro by 1.8-MHz pulsed ultrasound. *Ultrasound in medicine & biology* 35, 523–526.

Fadel PJ, Stromstad M, Hansen J, Sander M, Horn K, Ogoh S, Smith ML, Secher NH & Raven PB (2001). Arterial baroreflex control of sympathetic nerve activity during acute hypotension: effect of fitness. *Am J Physiol Heart Circ Physiol* 280, H2524–32.

Fan J, Burgess K, Basnyat R, Thomas K, Peebles K, Lucas S, Lucas R, Donnelly J, Cotter J & Ainslie P (2010a). Influence of high altitude on cerebrovascular and ventilatory responsiveness to CO2. *J Physiol (Lond)* 588, 539–549.

Fan JL, Burgess KR, Thomas KN, Peebles KC, Lucas SJ, Lucas RA, Cotter JD & Ainslie PN (2010b). Influence of indomethacin on ventilatory and cerebrovascular responsiveness to CO2 and breathing stability: the influence of PCO2 gradients. *Am J Physiol Regul Integr Comp Physiol* 298, R1648–58.

Fan J-L, Cotter JD, Lucas RAI, Thomas K, Wilson L & Ainslie PN (2008). Human cardiorespiratory and cerebrovascular function during severe passive hyperthermia: effects of mild hypohydration. *Journal of applied physiology (Bethesda, Md : 1985)* 105, 433–445.

Fortune JB, Bock D, Kupinski AM, Stratton HH, Shah DM & Feustel PJ (1992). Human cerebrovascular response to oxygen and carbon dioxide as determined by internal carotid artery duplex scanning. *J Trauma* 32, 618–27; discussion 627-8.

Galvin SD, Celi LA, Thomas KN, Clendon TR, Galvin IE, Bunton RW & Ainslie PN (2010). Effects of age and coronary artery disease on cerebrovascular reactivity to carbon dioxide in humans. *Anaesth Intensive Care* 38, 710–717.

Gerriets T, Postert T, Goertler M, Stolz E, Schlachetzki F, Sliwka U, Seidel G, Weber S & Kaps M (2000). DIAS I: duplex-sonographic assessment of the cerebrovascular status in acute stroke. A useful tool for future stroke trials. *Stroke* 31, 2342–2345.

Girouard H & Iadecola C (2006). Neurovascular coupling in the normal brain and in hypertension, stroke, and Alzheimer disease. *J Appl Physiol* 100, 328–335.

Green DJ, Jones H, Thijssen D, Cable NT & Atkinson G (2011). Flow-mediated dilation and cardiovascular event prediction: does nitric oxide matter? *Hypertension* 57, 363–369.

Greenfield JC & Tindall GT (1968). Effect of norepinephrine, epinephrine, and angiotensin on blood flow in the internal carotid artery of man. *J Clin Invest* 47, 1672–1684.

Grubb RLJ, Raichle ME, Eichling JO & Ter-Pogossian MM (1974). The effects of changes in PaCO2 on cerebral blood volume, blood flow, and vascular mean transit time. *Stroke* 5, 630–639.

Hamner JW, Cohen MA, Mukai S, Lipsitz LA & Taylor JA (2004). Spectral indices of human cerebral blood flow control: responses to augmented blood pressure oscillations. *The Journal of Physiology* 559, 965–973.

Harper AM & Glass HI (1965). Effect of alterations in the arterial carbon dioxide tension on the blood flow through the cerebral cortex at normal and low arterial blood pressures. *J Neurol Neurosurg Psychiatr* 28, 449–452.

Hauge A, Thoresen M & Walloe L (1980). Changes in cerebral blood flow during hyperventilation and CO2-breathing measured transcutaneously in humans by a bidirectional, pulsed, ultrasound Doppler blood velocitymeter. *Acta Physiol Scand* 110, 167–173.

Hellström G, Fischer-Colbrie W, Wahlgren NG & Jogestrand T (1996). Carotid artery blood flow and middle cerebral artery blood flow velocity during physical exercise. *Journal of applied physiology (Bethesda, Md : 1985)* 81, 413–418.

Helton WS, Hollander TD, Warm JS, Tripp LD, Parsons K, Matthews G, Dember WN, Parasuraman R & Hancock PA (2007). The abbreviated vigilance task and cerebral hemodynamics. *Jounral of Clinical and Experimental Neurophysiology* 29, 545–552.

Hendrikse J, van der Grond J, Lu H, van Zijl PC & Golay X (2004). Flow territory mapping of the cerebral arteries with regional perfusion MRI. *Stroke* 35, 882–887.

Hetzel A, Reinhard M, Guschlbauer B & Braune S (2003). Challenging cerebral autoregulation in patients with preganglionic autonomic failure. *Clin Auton Res* 13, 27–35.

Hoksbergen AW, Fulesdi B, Legemate DA & Csiba L (2000). Collateral configuration of the circle of Willis: transcranial color-coded duplex ultrasonography and comparison with postmortem anatomy. *Stroke* 31, 1346–1351.

Hossmann KA (1994). Viability thresholds and the penumbra of focal ischemia. *Ann Neurol* 36, 557–565.

Hubel DH & Wiesel TN (2005). Oxford University Press, New York.

Iadecola C & Nedergaard M (2007). Glial regulation of the cerebral microvasculature. *Nat Neurosci* 10, 1369–1376.

Immink R, Van Den Born B, Van Montfrans G, Kim Y, Hollmann M & Van Lieshout J (2008). Cerebral Hemodynamics During Treatment With Sodium Nitroprusside Versus Labetalol in Malignant Hypertension. *Hypertension* 52, 236–240.

Ito S, Mardimae A, Han J, Duffin J, Wells G, Fedorko L, Minkovich L, Katznelson R, Meineri M, Arenovich T, Kessler C & Fisher JA (2008). Non-invasive prospective targeting of arterial P(CO2) in subjects at rest. *J Physiol (Lond)* 586, 3675–3682.

Jakovcevic D & Harder DR (2007). Role of astrocytes in matching blood flow to neuronal activity. *Curr Top Dev Biol* 79, 75–97.

Jegede AB, Rosado-Rivera D, Bauman WA, Cardozo CP, Sano M, Moyer JM, Brooks M & Wecht JM (2009). Cognitive performance in hypotensive persons with spinal cord injury. *Clin Auton Res* .

Kamm C, Nagele T, Mittelbronn M, Schoning M, Melms A, Gasser T & Schols L (2008). Primary central nervous system vasculitis in a child mimicking parasitosis. *J Neurol* 255, 130–132.

Kehrer M, Blumenstock G, Ehehalt S, Goelz R, Poets C & Schoning M (2005). Development of cerebral blood flow volume in preterm neonates during the first two weeks of life. *Pediatr Res* 58, 927–930.

Kehrer M & Schoning M (2009). Quantitative sonographic measurement of cerebral blood flow volume in infants with periventricular leukomalacia. *Brain Dev* 31, 473.

Kety S & Schmidt C (1945). The determination of cerebral blood flow in man by the use of nitrous oxide in low concentrations. *Americal Journal of Physiology* 33–52.

Kety SS (1999). Mental illness and the sciences of brain and behavior. *Nat Med* 5, 1113–1116.

Kety SS & Schmidt CF (1948). The nitrous oxide method for the quantitative determination of cerebral blood flow in man; theory, procedure and normal values. *J Clin Invest* 27, 476–483.

Klingelhöfer J, Matzander G, Sander D, Schwarze J, Boecker H & Bischoff C (1997). Assessment of functional hemispheric asymmetry by bilateral simultaneous cerebral blood flow velocity monitoring. *J Cereb Blood Flow Metab* 17, 577–585.

Knecht S, Deppe M, Bäcker M, Ringelstein EB & Henningsen H (1997). Regional cerebral blood flow increases during preparation for and processing of sensory stimuli. *Experimental brain research Experimentelle Hirnforschung Expérimentation cérébrale* 116, 309–314.

Knecht S, Deppe M, Ebner A, Henningsen H, Huber T, Jokeit H & Ringelstein EB (1998a). Noninvasive determination of language lateralization by functional transcranial Doppler sonography: a comparison with the Wada test. *Stroke* 29, 82–86.

Knecht S, Deppe M, Ringelstein EB, Wirtz M, Lohmann H, Dräger B, Huber T & Henningsen H (1998b). Reproducibility of functional transcranial Doppler sonography in determining hemispheric language lateralization. *Stroke* 29, 1155–1159.

Kolb JC, Ainslie PN, Ide K & Poulin MJ (2004). Protocol to measure acute cerebrovascular and ventilatory responses to isocapnic hypoxia in humans. *Respiratory physiology & neurobiology* 141, 191–199.

Krejza J, Mariak Z, Melhem ER & Bert RJ (2000). A guide to the identification of major cerebral arteries with transcranial color Doppler sonography. *AJR Am J Roentgenol* 174, 1297–1303.

Kuker W, Gaertner S, Nagele T, Dopfer C, Schoning M, Fiehler J, Rothwell PM & Herrlinger U (2008). Vessel wall contrast enhancement: a diagnostic sign of cerebral vasculitis. *Cerebrovasc Dis* 26, 23–29.

Lassen NA (1959). Cerebral blood flow and oxygen consumption in man. *Physiol Rev* 39, 183–238.

Lassen NA, HOEDT-RASMUSSEN K, SORENSEN SC, SKINHOJ E, CRONQUIST S, BODFORSS B & INGVAR DH (1963). REGIONAL CEREBRAL BLOOD FLOW IN MAN DETERMINED BY KRYPTON. *Neurology* 13, 719–727.

Leopold PW, Shandall AA, Feustel P, Corson JD, Shah DM, Popp AJ, Fortune JB, Leather RP & Karmody AM (1987). Duplex scanning of the internal carotid artery: an assessment of cerebral blood flow. *Br J Surg* 74, 630–633.

Lohmann H, Ringelstein EB & Knecht S (2006). Functional transcranial Doppler sonography. *Frontiers of neurology and neuroscience* 21, 251–260.

Lucas SJ, Tzeng YC, Galvin SD, Thomas KN, Ogoh S & Ainslie PN (2010a). Influence of changes in blood pressure on cerebral perfusion and oxygenation. *Hypertension* 55, 698–705.

Lucas SJ, Burgess KR, Thomas KN, Donnelly J, Peebles KC, Lucas RA, Fan JL, Basnyat R, Cotter JD & Ainslie PN (2010b). Alterations in cerebral blood flow and cerebrovascular reactivity during 14 days at 5050 m. *J Physiol*

MacKenzie ET, McCulloch J, O'Kean M, Pickard JD & Harper AM (1976). Cerebral circulation and norepinephrine: relevance of the blood-brain barrier. *Am J Physiol* 231, 483–488.

Mahony PJ, Panerai RB, Deverson ST, Hayes PD & Evans DH (2000). Assessment of the thigh cuff technique for measurement of dynamic cerebral autoregulation. *Stroke* 31, 476–480.

Mandell DM, Han JS, Poublanc J, Crawley AP, Kassner A, Fisher JA & Mikulis DJ (2008). Selective reduction of blood flow to white matter during hypercapnia corresponds with leukoaraiosis. *Stroke* 39, 1993–1998.

Markus H & Cullinane M (2001). Severely impaired cerebrovascular reactivity predicts stroke and TIA risk in patients with carotid artery stenosis and occlusion. *Brain* 124, 457–467.

Markus HS & Boland M (1992). "Cognitive activity" monitored by non-invasive measurement of cerebral blood flow velocity and its application to the investigation of cerebral dominance. *Cortex* 28, 575–581.

Markus HS & Punter M (2005). Can transcranial Doppler discriminate between solid and gaseous microemboli? Assessment of a dual-frequency transducer system. *Stroke* 36, 1731–1734.

Martin PJ, Evans DH & Naylor AR (1995). Measurement of blood flow velocity in the basal cerebral circulation: advantages of transcranial color-coded sonography over conventional transcranial Doppler. *J Clin Ultrasound* 23, 21–26.

Mascia L, Fedorko L, terBrugge K, Filippini C, Pizzio M, Ranieri VM & Wallace MC (2003). The accuracy of transcranial Doppler to detect vasospasm in patients with aneurysmal subarachnoid hemorrhage. *Intensive Care Med* 29, 1088–1094.

McCalden TA, Eidelman BH & Mendelow AD (1977). Barrier and uptake mechanisms in the cerebrovascular response to noradrenaline. *Am J Physiol* 233, H458–65.

Mitchell J (2005). The vertebral artery: a review of anatomical, histopathological and functional factors influencing blood flow to the hindbrain. *Physiother Theory Pract* 21, 23–36.

Miyazaki M & Kato K (1965). Measurement of cerebral blood flow by ultrasonic Doppler technique; hemodynamic comparison of right and left carotid artery in patients with hemiplegia. *Jpn Circ J* 29, 383–386.

Mosso A (1880). Sulla circolazione del cervello dell'uomo. *Att R Accad Lincei* 5, 237–358.

Murrell C, Cotter J, George K, Shave R, Wilson L, Thomas K, Williams M, Lowe T & Ainslie P (2009). Influence of age on syncope following prolonged exercise; differential responses but similar orthostatic intolerance. *J Physiol (Lond)* 1–11.

Murrell C, Wilson L, Cotter JD, Lucas S, Ogoh S, George K & Ainslie PN (2007). Alterations in autonomic function and cerebral hemodynamics to orthostatic challenge following a mountain marathon. *J Appl Physiol* 103, 88–96.

Nabavi DG, Droste DW, Schulte-Altedorneburg G, Kemeny V, Panzica M, Weber S & Ringelstein EB (1999). Diagnostic benefit of echocontrast enhancement for the insufficient transtemporal bone window. *J Neuroimaging* 9, 102–107.

Njemanze PC (1991). Cerebral lateralization in linguistic and nonlinguistic perception: analysis of cognitive styles in the auditory modality. *Brain and language* 41, 367–380.

Nöth U, Kotajima F, Deichmann R, Turner R & Corfield DR (2008). Mapping of the cerebral vascular response to hypoxia and hypercapnia using quantitative perfusion MRI at 3 T. *NMR in biomedicine* 21, 464–472.

Nuttall GA, Cook DJ, Fulgham JR, Oliver WC & Proper JA (1996). The relationship between cerebral blood flow and transcranial Doppler blood flow velocity during hypothermic cardiopulmonary bypass in adults. *Anesth Analg* 82, 1146–1151.

Ogoh S & Ainslie PN (2009a). Regulatory mechanisms of cerebral blood flow during exercise: new concepts. *Exercise and sport sciences reviews* 37, 123–129.

Ogoh S & Ainslie PN (2009b). Cerebral blood flow during exercise: mechanisms of regulation. *J Appl Physiol* 107, 1370–1380.

Ogoh S, Brothers R, Jeschke M, Secher N & Raven P (2010). Estimation of cerebral vascular tone during exercise; evaluation by critical closing pressure in humans. *Exp Physiol* 95, 678–685.

Ogoh S, Fadel PJ, Nissen P, Jans Ø, Selmer C, Secher NH & Raven PB (2003). Baroreflex-mediated changes in cardiac output and vascular conductance in response to alterations in carotid sinus pressure during exercise in humans. *J Physiol (Lond)* 550, 317–324.

Ogoh S, Fisher JP, Fadel PJ & Raven PB (2007). Increases in central blood volume modulate carotid baroreflex resetting during dynamic exercise in humans. *J Physiol (Lond)* 581, 405–418.

Ogoh S, Tzeng YC, Lucas SJ, Galvin SD & Ainslie PN (2009). Influence of baroreflex-mediated tachycardia on the regulation of dynamic cerebral perfusion during acute hypotension in humans. *J Physiol (Lond)* .

Orlandi G & Murri L (1996). Transcranial Doppler assessment of cerebral flow velocity at rest and during voluntary movements in young and elderly healthy subjects. *Int J Neurosci* 84, 45–53.

Padayachee TS, Parsons S, Theobold R, Linley J, Gosling RG & Deverall PB (1987). The detection of microemboli in the middle cerebral artery during cardiopulmonary bypass: a transcranial Doppler ultrasound investigation using membrane and bubble oxygenators. *Ann Thorac Surg* 44, 298–302.

Panerai R (2009). Complexity of the human cerebral circulation. *Philosophical Transactions of the Royal Society A: Mathematical, Physical and Engineering Sciences* 367, 1319–1336.

Panerai RB (2003). The critical closing pressure of the cerebral circulation. *Medical engineering & physics* 25, 621–632.

Panerai RB (2008). Cerebral autoregulation: from models to clinical applications. *Cardiovascular engineering (Dordrecht, Netherlands)* 8, 42–59.

Panerai RB, Dawson SL, Eames PJ & Potter JF (2001). Cerebral blood flow velocity response to induced and spontaneous sudden changes in arterial blood pressure. *Am J Physiol Heart Circ Physiol* 280, H2162–74.

Panerai RB, Dawson SL & Potter JF (1999a). Linear and nonlinear analysis of human dynamic cerebral autoregulation. *Am J Physiol* 277, H1089–99.

Panerai RB, Deverson ST, Mahony P, Hayes P & Evans DH (1999b). Effects of CO2 on dynamic cerebral autoregulation measurement. *Physiological measurement* 20, 265–275.

Panerai RB, Rennie JM, Kelsall AW & Evans DH (1998). Frequency-domain analysis of cerebral autoregulation from spontaneous fluctuations in arterial blood pressure. *Medical & biological engineering & computing* 36, 315–322.

Peebles KC, Richards AM, Celi L, McGrattan K, Murrell CJ & Ainslie PN (2008). Human cerebral arteriovenous vasoactive exchange during alterations in arterial blood gases. *J Appl Physiol* 105, 1060–1068.

Pickkers P, Hughes AD, Russel FG, Thien T & Smits P (2001). In vivo evidence for K(Ca) channel opening properties of acetazolamide in the human vasculature. *Br J Pharmacol* 132, 443–450.

Piechnik SK, Chiarelli PA & Jezzard P (2008). Modelling vascular reactivity to investigate the basis of the relationship between cerebral blood volume and flow under CO2 manipulation. *Neuroimage* 39, 107–118.

Postert T, Federlein J, Przuntek H & Buttner T (1997). Insufficient and absent acoustic temporal bone window: potential and limitations of transcranial contrast-enhanced color-coded sonography and contrast-enhanced power-based sonography. *Ultrasound Med Biol* 23, 857–862.

Powers J, Averkiou M & Bruce M (2009). Principles of cerebral ultrasound contrast imaging. *Cerebrovasc Dis* 27 Suppl 2, 14–24.

Querido JS & Sheel AW (2007). Regulation of cerebral blood flow during exercise. *Sports medicine (Auckland, NZ)* 37, 765–782.

Rasulo FA, De Peri E & Lavinio A (2008). Transcranial Doppler ultrasonography in intensive care. *European journal of anaesthesiology Supplement* 42, 167–173.

Reichmuth K, Dopp JM, Barczi SR, Skatrud JB, Wojdyla P, Hayes Jr D & Morgan BJ (2009). Impaired Vascular Regulation in Patients with Obstructive Sleep Apnea: Effects of CPAP Treatment. *Am J Respir Crit Care Med* .

Ringelstein EB, Droste DW, Babikian VL, Evans DH, Grosset DG, Kaps M, Markus HS, Russell D & Siebler M (1998). Consensus on microembolus detection by TCD. International Consensus Group on Microembolus Detection. *Stroke* 29, 725–729.

Ringelstein EB, Kahlscheuer B, Niggemeyer E & Otis SM (1990). Transcranial Doppler sonography: anatomical landmarks and normal velocity values. *UMB* 16, 745–761.

Robbins PA, Swanson GD & Howson MG (1982). A prediction-correction scheme for forcing alveolar gases along certain time courses. *Journal of applied physiology: respiratory, environmental and exercise physiology* 52, 1353–1357.

Rodriguez RA, Nathan HJ, Ruel M, Rubens F, Dafoe D & Mesana T (2009). A method to distinguish between gaseous and solid cerebral emboli in patients with prosthetic heart valves. *European journal of cardio-thoracic surgery : official journal of the European Association for Cardio-thoracic Surgery* 35, 89–95.

Ropper AH, Kehne SM & Wechsler L (1987). Transcranial Doppler in brain death. *Neurology* 37, 1733–1735.

Rosengarten B, Aldinger C, Kaufmann A & Kaps M (2002a). Neurovascular coupling remains unaffected by glyceryl trinitrate. *Cerebrovasc Dis* 14, 58–60.

Rosengarten B, Dost A, Kaufmann A, Gortner L & Kaps M (2002b). Impaired cerebrovascular reactivity in type 1 diabetic children. *Diabetes Care* 25, 408–410.

Rosengarten B, Paulsen S, Molnar S, Kaschel R, Gallhofer B & Kaps M (2007). Activation-flow coupling differentiates between vascular and Alzheimer type of dementia. *J Neurol Sci* 257, 149–154.

Rosengarten B, Spiller A, Aldinger C & Kaps M (2003). Control system analysis of visually evoked blood flow regulation in humans under normocapnia and hypercapnia. *European journal of ultrasound : official journal of the European Federation of Societies for Ultrasound in Medicine and Biology* 16, 169–175.

Sato K, Ogoh S, Hirasawa A, Oue A & Sadamoto T (2011). The distribution of blood flow in the carotid and vertebral arteries during dynamic exercise in humans. *J Physiol (Lond)* .

Sato K & Sadamoto T (2010). Different blood flow responses to dynamic exercise between internal carotid and vertebral arteries in women. *J Appl Physiol* 109, 864–869.

Scheel P, Ruge C, Petruch UR & Schoning M (2000a). Color duplex measurement of cerebral blood flow volume in healthy adults. *Stroke* 31, 147–150.

Scheel P, Ruge C & Schoning M (2000b). Flow velocity and flow volume measurements in the extracranial carotid and vertebral arteries in healthy adults: reference data and the effects of age. *Ultrasound Med Biol* 26, 1261–1266.

Schnittger C, Johannes S, Arnavaz A & Münte TF (1997). Blood flow velocity changes in the middle cerebral artery induced by processing of hierarchical visual stimuli. *Neuropsychologia* 35, 1181–1184.

Schnittger C, Johannes S & Münte TF (1996). Transcranial Doppler assessment of cerebral blood flow velocity during visual spatial selective attention in humans. *Neuroscience Letters* 214, 41–44.

Schoning M & Hartig B (1996). Age dependence of total cerebral blood flow volume from childhood to adulthood. *J Cereb Blood Flow Metab* 16, 827–833.

Schoning M, Scheel P, Holzer M, Fretschner R & Will BE (2005a). Volume measurement of cerebral blood flow: assessment of cerebral circulatory arrest. *Transplantation* 80, 326–331.

Schoning M, Scheel P, Holzer M, Fretschner R & Will BE (2005b). Volume measurement of cerebral blood flow: assessment of cerebral circulatory arrest. *Transplantation* 80, 326–331.

Schoning M, Walter J & Scheel P (1994). Estimation of cerebral blood flow through color duplex sonography of the carotid and vertebral arteries in healthy adults. *Stroke* 25, 17–22.

Serrador JM, Picot PA, Rutt BK, Shoemaker JK & Bondar RL (2000). MRI measures of middle cerebral artery diameter in conscious humans during simulated orthostasis. *Stroke* 31, 1672–1678.

Serrador JM, Sorond FA, Vyas M, Gagnon M, Iloputaife ID & Lipsitz LA (2005). Cerebral pressure-flow relations in hypertensive elderly humans: transfer gain in different frequency domains. *J Appl Physiol* 98, 151–159.

Settakis G, Molnár C, Kerényi L, Kollár J, Legemate D, Csiba L & Fülesdi B (2003). Acetazolamide as a vasodilatory stimulus in cerebrovascular diseases and in conditions affecting the cerebral vasculature. *Eur J Neurol* 10, 609–620.

Silvestrini M, Caltagirone C, Cupini LM, Matteis M, Troisi E & Bernardi G (1993). Activation of healthy hemisphere in poststroke recovery. A transcranial Doppler study. *Stroke* 24, 1673–1677.

Silvestrini M, Troisi E, Matteis M, Cupini LM & Caltagirone C (1995). Involvement of the healthy hemisphere in recovery from aphasia and motor deficit in patients with cortical ischemic infarction: a transcranial Doppler study. *Neurology* 45, 1815–1820.

Silvestrini M, Troisi E, Matteis M, Razzano C & Caltagirone C (1998). Correlations of flow velocity changes during mental activity and recovery from aphasia in ischemic stroke. *Neurology* 50, 191–195.

Silvestrini M, Vernieri F, Pasqualetti P, Matteis M, Passarelli F, Troisi E & Caltagirone C (2000). Impaired cerebral vasoreactivity and risk of stroke in patients with asymptomatic carotid artery stenosis. *JAMA* 283, 2122–2127.

Sitzer M, Knorr U & Seitz RD (1994). cerebral hemodynamics during sensorimotor activation in humans. *Journal of Applied Physiology* 77, 2804–2811.

Slessarev M, Han J, Mardimae A, Prisman E, Preiss D, Volgyesi G, Ansel C, Duffin J & Fisher J (2007). Prospective targeting and control of end-tidal CO2 and O2 concentrations. *The Journal of Physiology* 581, 1207–1219.

Sloan MA, Alexandrov AV, Tegeler CH, Spencer MP, Caplan LR, Feldmann E, Wechsler LR, Newell DW, Gomez CR, Babikian VL, Lefkowitz D, Goldman RS, Armon C, Hsu CY & Goodin DS (2004). Assessment: transcranial Doppler ultrasonography: report of the Therapeutics and Technology Assessment Subcommittee of the American Academy of Neurology. *Neurology* 62, 1468–1481.

Smith ML, Beightol LA, Fritsch-Yelle JM, Ellenbogen KA, Porter TR & Eckberg DL (1996). Valsalva's maneuver revisited: a quantitative method yielding insights into human autonomic control. *Am J Physiol* 271, H1240–9.

Smyth HS, Sleight P & Pickering GW (1969). Reflex regulation of arterial pressure during sleep in man. A quantitative method of assessing baroreflex sensitivity. *Circ Res* 24, 109–121.

Sorond FA, Khavari R, Serrador JM & Lipsitz LA (2005). Regional cerebral autoregulation during orthostatic stress: age-related differences. *J Gerontol A Biol Sci Med Sci* 60, 1484–1487.

Strandness DEJ (1985). Echo-Doppler (duplex) ultrasonic scanning. *J Vasc Surg* 2, 341–344.

Stroobant N & Vingerhoets G (2000). Transcranial Doppler ultrasonography monitoring of cerebral hemodynamics during performance of cognitive tasks: a review. *Neuropsychology review* 10, 213–231.

Taylor JA, Carr DL, Myers CW & Eckberg DL (1998). Mechanisms underlying very-low-frequency RR-interval oscillations in humans. *Circulation* 98, 547–555.

ter Minassian A, Melon E, Leguerinel C, Lodi CA, Bonnet F & Beydon L (1998). Changes in cerebral blood flow during PaCO2 variations in patients with severe closed head injury: comparison between the Fick and transcranial Doppler methods. *J Neurosurg* 88, 996–1001.

Thie A, Carvajal-Lizano M, Schlichting U, Spitzer K & Kunze K (1992). Multimodal tests of cerebrovascular reactivity in migraine: a transcranial Doppler study. *J Neurol* 239, 338–342.

Thomas KN, Cotter JD, Galvin SD, Williams MJ, Willie CK & Ainslie PN (2009). Initial orthostatic hypotension is unrelated to orthostatic tolerance in healthy young subjects. *J Appl Physiol* 107, 506–517.

Tiecks FP, Douville C, Byrd S, Lam AM & Newell DW (1996). Evaluation of impaired cerebral autoregulation by the Valsalva maneuver. *Stroke* 27, 1177–1182.

Tiecks FP, Lam AM, Aaslid R & Newell DW (1995a). Comparison of static and dynamic cerebral autoregulation measurements. *Stroke* 26, 1014–1019.

Tiecks FP, Lam AM, Matta BF, Strebel S, Douville C & Newell DW (1995b). Effects of the Valsalva Maneuver on Cerebral Circulation in Healthy Adults : A Transcranial Doppler Study. *Stroke* 26, 1386–1392.

Troisi E, Silvestrini M, Matteis M, Monaldo BC, Vernieri F & Caltagirone C (1999). Emotion-related cerebral asymmetry: hemodynamics measured by functional ultrasound. *J Neurol* 246, 1172–1176.

Tsivgoulis G, Alexandrov AV & Sloan MA (2009). Advances in transcranial Doppler ultrasonography. *Current neurology and neuroscience reports* 9, 46–54.

Tzeng YC, Lucas SJ, Atkinson G, Willie CK & Ainslie PN (2010a). Fundamental relationships between arterial baroreflex sensitivity and dynamic cerebral autoregulation in humans. *J Appl Physiol* 108, 1162–1168.

Tzeng YC, Willie CK, Atkinson G, Lucas SJ, Wong A & Ainslie PN (2010b). Cerebrovascular regulation during transient hypotension and hypertension in humans. *Hypertension* 56, 268–273.

Tzeng YC, Willie CK & Ainslie PN (2010c). Baroreflex, cerebral perfusion, and stroke: integrative physiology at its best. *Stroke* 41, e429.

Valdueza JM, Balzer JO, Villringer A, Vogl TJ, Kutter R & Einhäupl KM (1997). Changes in blood flow velocity and diameter of the middle cerebral artery during hyperventilation: assessment with MR and transcranial Doppler sonography. *AJNR American journal of neuroradiology* 18, 1929–1934.

Vernieri F, Pasqualetti P, Matteis M, Passarelli F, Troisi E, Rossini PM, Caltagirone C & Silvestrini M (2001). Effect of collateral blood flow and cerebral vasomotor reactivity on the outcome of carotid artery occlusion. *Stroke* 32, 1552–1558.

Widder B, Kleiser B & Krapf H (1994). Course of cerebrovascular reactivity in patients with carotid artery occlusions. *Stroke* 25, 1963–1967.

Wijnhoud AD, Koudstaal PJ & Dippel DW (2006). Relationships of transcranial blood flow Doppler parameters with major vascular risk factors: TCD study in patients with a

recent TIA or nondisabling ischemic stroke. *Journal of clinical ultrasound : JCU* 34, 70–76.

Willie CK, Cowan EC, Ainslie PN, Taylor CE, Smith KJ, Sin PYW & Tzeng YC (2011a). Neurovascular coupling and distribution of cerebral blood flow during exercise. *Journal of Neuroscience Methods* 198, 270–273.

Willie CK, Colino FL, Bailey DM, Tzeng YC, Binsted G, Jones LW, Haykowsky MJ, Bellapart J, Ogoh S, Smith KJ, Smirl JD, Day TA, Lucas SJ, Eller LK & Ainslie PN (2011b). Utility of transcranial Doppler ultrasound for the integrative assessment of cerebrovascular function. *Journal of Neuroscience Methods* 196, 221–237.

Wilson LC, Cotter JD, Fan JL, Lucas RA, Thomas KN & Ainslie PN (2010). Cerebrovascular reactivity and dynamic autoregulation in tetraplegia. *Am J Physiol Regul Integr Comp Physiol* 298, R1035–42.

Wintermark M, Sesay M, Barbier E, Borbély K, Dillon WP, Eastwood JD, Glenn TC, Grandin CB, Pedraza S, Soustiel JF, Nariai T, Zaharchuk G, Caillé JM, Dousset V & Yonas H (2005). Comparative overview of brain perfusion imaging techniques. *Stroke* 36, e83–99.

Woods T, Harmann L, Purath T, Ramamurthy S, Subramanian S, Jackson S & Tarima S (2010). Small- and Moderate-Size Right-to-Left Shunts Identified by Saline Contrast Echocardiography Are Normal and Unrelated to Migraine Headache. *Chest* 138, 264–269.

Xie A, Skatrud JB, Khayat R, Dempsey JA, Morgan B & Russell D (2005). Cerebrovascular response to carbon dioxide in patients with congestive heart failure. *Am J Respir Crit Care Med* 172, 371–378.

Zagorac D, Yamaura K, Zhang C, Roman RJ & Harder DR (2005). The effect of superoxide anion on autoregulation of cerebral blood flow. *Stroke* 36, 2589–2594.

Zhang R, Zuckerman JH, Giller CA & Levine BD (1998). Transfer function analysis of dynamic cerebral autoregulation in humans. *Am J Physiol* 274, H233–41.

Zhang R, Zuckerman JH, Iwasaki K, Wilson TE, Crandall CG & Levine BD (2002). Autonomic neural control of dynamic cerebral autoregulation in humans. *Circulation* 106, 1814–1820.

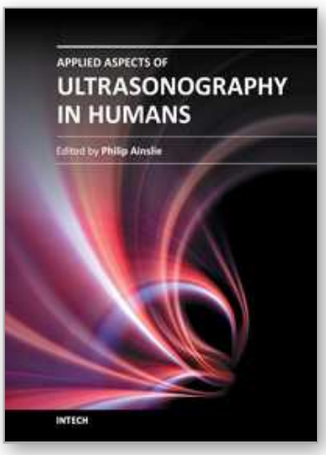

Applied Aspects of Ultrasonography in Humans
Edited by Prof. Philip Ainslie

ISBN 978-953-51-0522-0
Hard cover, 190 pages
Publisher InTech
Published online 25, April, 2012
Published in print edition April, 2012

Written by international experts, this publication provides the reader with the present knowledge and future research directions of diagnostic and therapeutic ultrasound and spectroscopy. Focused topics include Duplex ultrasound, transcranial color Duplex, MRA guided Doppler ultrasonography and near-infrared spectroscopy. New directions in the use and application of transcranial and color Duplex ultrasound are provided, as well as the use of ultrasound and arterial stiffness for measuring human vascular health and circulatory control. Novel use of ultrasound for the detection of intra-cardiac and intra-pulmonary shunts is also described along with its utility for the assessment of gastric regulation and emptying.

INTECH
open science | open minds

InTech Europe
University Campus STeP Ri
Slavka Krautzeka 83/A
51000 Rijeka, Croatia
Phone: +385 (51) 770 447
Fax: +385 (51) 686 166
www.intechopen.com

InTech China
Unit 405, Office Block, Hotel Equatorial Shanghai
No.65, Yan An Road (West), Shanghai, 200040, China
中国上海市延安西路65号上海国际贵都大饭店办公楼405单元
Phone: +86-21-62489820
Fax: +86-21-62489821

IntechOpen